2. EXPLANATORY NOTES[1]

Shipboard Scientific Party[2]

INTRODUCTION

In this chapter, we have assembled information that will help the reader understand the observations on which our preliminary conclusions have been based and also will help the interested investigator to select samples for further analysis. This information concerns only shipboard operations and analyses described in the site reports in the *Initial Reports* volume of the Leg 152 *Proceedings of the Ocean Drilling Program.* Methods used by various investigators for shore-based analyses of Leg 152 data will be described in the individual scientific contributions to be published in the *Scientific Results* volume.

AUTHORSHIP OF SITE CHAPTERS

The separate sections of the site chapters were written by the following shipboard scientists (authors are listed in alphabetical order):

Site Summary: Hans Christian Larsen, Andrew Saunders
Background and Scientific Objectives: Hans Christian Larsen, Andrew Saunders
Operations: Ron Grout, Peter Clift
Site Geophysics: Hans Christian Larsen, Holger Lykke-Andersen
Lithostratigraphy: James Begét, Peter Clift, Mary Anne Holmes, Christian Lacasse, Saneatsu Saito, Tracy Vallier, Reinhard Werner
Biostratigraphy: Naoki Nemoto, Silvia Spezzaferri, Wuchang Wei
Paleomagnetism: Jason Ali, Koji Fukuma, Didier Vandamme
Igneous Petrology and Geochemistry: Alain Demant, Godfrey Fitton, Miranda Fram, Lotte Melchior Larsen, Christopher Sinton
Organic Geochemistry: Rainer Stax
Inorganic Geochemistry: Joris Gieskes
Physical Properties: Jonathan Hunt, Martin Morrison, Nilgün Okay
Downhole Measurements: Hervé Cambray, Holger Lykke-Andersen
Underway Geophysics: Hans Christian Larsen, Holger Lykke-Andersen
Summary and Conclusions: Hans Christian Larsen, Andrew Saunders

Following the text of all site chapters, in a special section called "Cores," are summary core descriptions ("barrel sheets") and photographs of each core.

DRILLING CHARACTERISTICS

Because water circulation through the drill pipe is an open system, cuttings are lost onto the seafloor and cannot be examined. The properties of the uncored or unrecovered intervals may be inferred from seismic data, from wireline-logging results, and from an examination of the behavior of the drill string, as observed and recorded on the drilling platform. Typically, the harder a layer, the slower and more difficult it is to penetrate. A number of other factors may determine the rate of penetration; thus, it is not always possible to relate drilling time directly to the hardness of the layers. Bit weight and revolutions per minute, recorded on the drilling recorder, also influence penetration rate.

Drilling Deformation

When split, many cores show signs of significant sediment disturbance, including the concave-downward appearance of originally horizontal bands, haphazard mixing of lumps of different lithologies (mainly at the tops of cores), and the near-fluid state of some sediments recovered from tens to hundreds of meters below the seafloor. Core deformation probably occurs during cutting, retrieval (with accompanying changes in pressure and temperature), and core handling on deck.

SHIPBOARD SCIENTIFIC PROCEDURES

Numbering of Sites, Holes, Cores, and Samples

ODP drill sites are numbered consecutively and refer to one or more holes drilled while the ship was positioned over one acoustic beacon. Multiple holes may be drilled at a single site by pulling the drill pipe above the seafloor (out of the hole), moving the ship some distance from the previous hole, and then drilling another hole.

For all ODP drill sites, a letter suffix distinguishes holes drilled at the same site. For example, the first hole to be drilled is assigned the site number modified by the suffix A, the second hole takes the site number and suffix B, and so forth. Note that this procedure differs slightly from that used by DSDP (Sites 1 through 624), but prevents ambiguity between site- and hole-number designations. It is important to distinguish among holes drilled at a site, because recovered sediments or rocks from different holes usually do not come from equivalent positions in the stratigraphic column.

The cored interval is measured in meters below seafloor (mbsf). Depths are measured during coring operations from the rig floor (Fig. 1) and are then corrected to sea level by subtracting the height of the rig floor, a measurement that varies during the cruise and that is quoted in the Site Summary at the start of each site chapter. The depth is also corrected to depth below seafloor by subtracting the depth below rig floor at which the bottom was first felt. The depth interval assigned to an individual core begins with the depth below the seafloor at which the coring began and extends to the depth where coring ended. For example, each coring interval is generally up to 9.5 m long, which is the length of a core barrel. Coring intervals may be shorter and may not necessarily be adjacent if separated by drilled intervals. In soft sediments, the drill string can be "washed ahead" with the core barrel in place, without recovering sediments. This is achieved by pumping water down the pipe at high pressure to wash the sediment out of the way of the bit and up the space between the drill pipe and the wall of the hole. If thin, hard, rock layers are present, then it is possible to get "spotty" sampling of these resistant layers within the washed interval and, thus, to have a cored interval greater than 9.5 m. When drilling

[1] Larsen, H.C., Saunders, A.D., Clift, P.D., et al., 1994. *Proc. ODP, Init. Repts.,* 152: College Station, TX (Ocean Drilling Program).
[2] Shipboard Scientific Party is as given in list of participants preceding the contents.

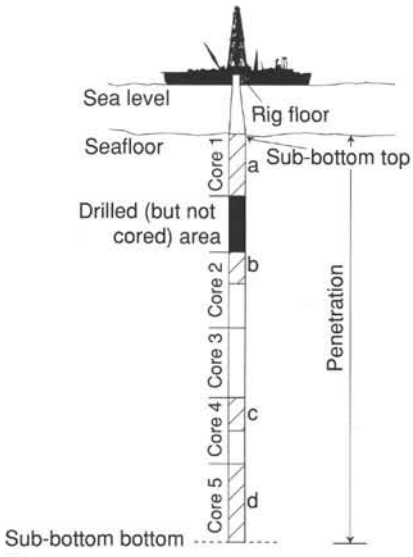

Bottom felt: distance from rig floor to seafloor
Total depth: distance from rig floor to bottom of hole (sub-bottom bottom)
Penetration: distance from seafloor to bottom of hole (sub-bottom bottom)
Number of cores: total of all cores recorded, including cores with no recovery
Total length of cored section: distance from sub-bottom top to sub-bottom bottom minus drilled (but not cored) areas in between
Total core recovered: total from adding a, b, c, and d in diagram
Core recovery (%): equals total core recovered divided by total length of cored section times 100

Figure 1. Diagram illustrating terms used when discussing core recovery and coring operations.

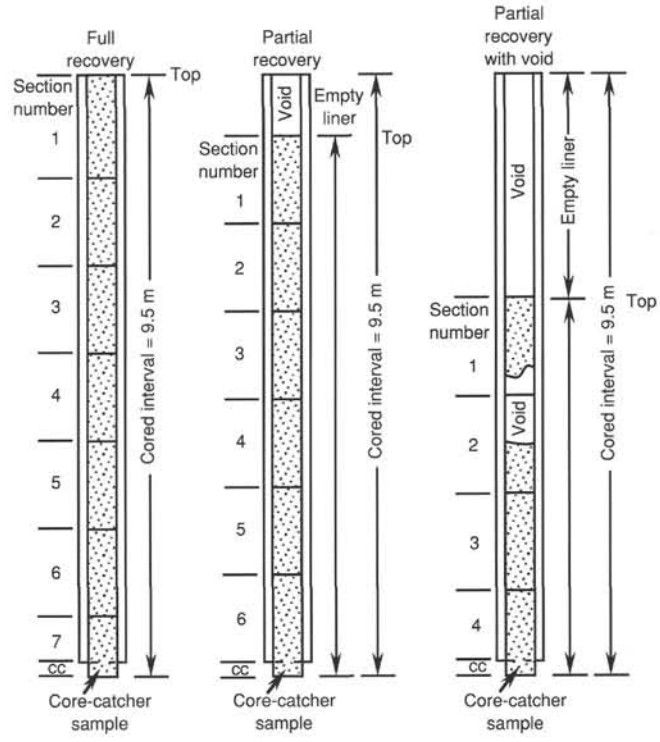

Figure 2. Examples of numbered sections.

hard rock, a center bit may replace the core barrel if it is necessary to drill without core recovery.

Cores taken from a hole are numbered serially from the top of the hole downward. Core numbers and their associated cored intervals in meters below seafloor usually are unique in a given hole; however, this may not be true if an interval is cored twice. Maximum recovery for a single core is 9.5 m of rock or sediment contained in a plastic liner (6.6 cm internal diameter) plus about 0.2 m (without a plastic liner) in the core catcher (Fig. 2). The core catcher is a device at the bottom of the core barrel that prevents the core from sliding out when the barrel is being retrieved from the hole. In certain situations (e.g., when coring gas-charged sediments that expand while being brought on deck), recovery may exceed the 9.5-m length cored.

A recovered core is divided into 1.5-m sections that are numbered serially from the top (Fig. 2). When full recovery is obtained, the sections are numbered from 1 through 7, with the last section possibly being shorter than 1.5 m (rarely, an unusually long core may require more than seven sections). In cases where the recovery is not complete, as many sections as necessary are used to accommodate the core; for example, 4 m of core would be divided into two 1.5-m sections and a 1-m section. If cores are fragmented (recovery less than 100%), sections are numbered serially and intervening sections are noted as void, whether or not shipboard scientists think that the fragments were contiguously in-situ. In rare cases, a section less than 1.5 m may be cut to preserve features of interest (e.g., lithologic contacts).

By convention, material recovered from the core catcher is placed below the last section when the core is described and is labeled core catcher (CC); in sedimentary cores, this is treated as a separate section. The core catcher is placed at the top of the cored interval in cases where material is recovered only in the core catcher. However, information supplied by the drillers or by other sources may allow for more precise interpretation as to the correct position of core-catcher material within an incompletely recovered cored interval.

When the recovered core is shorter than the cored interval, the top of the core is equated with the top of the cored interval by convention to achieve consistency when handling analytical data derived from the cores. Samples removed from the cores are designated by distance measured in centimeters from the top of the section to the top and bottom of each sample removed from that section.

A complete identification number for a sample consists of the following information: leg, site, hole, core number, core type, section number, piece number (for hard rock), and interval in centimeters measured from the top of the section. For example, a sample identification of "152-914A-25R-1, 10–12 cm" would be interpreted as representing a sample removed from the interval between 10 and 12 cm below the top of Section 1, Core 25 (R designates that this core was taken during rotary drilling) of Hole 914A during Leg 152.

All ODP core and sample identifiers indicate core type. The following abbreviations were used: R = rotary core barrel (RCB); H = hydraulic piston core (HPC; also referred to as APC, or advanced hydraulic piston core); P = pressure core barrel; X = extended core barrel (XCB); B = drill-bit recovery; C = center-bit recovery; I = in-situ water sample; S = sidewall sample; W = washed core recovery; and M = miscellaneous material. APC, XCB, and RCB cores were cut during Leg 152.

CORE HANDLING

Sediments

As soon as a core is retrieved on deck, a sample is taken from the core catcher and given to the paleontological laboratory for an initial age assessment. Then, the core is placed on a long horizontal rack, and gas samples may be taken by piercing the core liner and withdrawing gas into a vacuum-tube. Voids within the core are sought as sites for gas sampling. Some of the gas samples are stored for shore-based study; however, others are analyzed immediately as part of the ship-

board safety and pollution-prevention program. Next, the core is marked into section lengths, each section is labeled, and the core is cut into sections. Interstitial-water (IW) and physical-properties (PP) samples then are taken. In addition, some headspace gas samples are scraped from the ends of cut sections on the catwalk and sealed in glass vials for light hydrocarbon analysis. Each section then is sealed at the top and bottom by gluing on color-coded plastic caps, blue to identify the top of a section and clear to identify the bottom. A yellow cap is placed on the section ends from which a whole-round sample has been removed. These caps are usually attached to the liner by coating the end liner and the inside rim of the cap with acetone, and then the caps are taped to the liners.

Next, the cores are carried into the laboratory, where the sections again are labeled, using an engraver to mark the full designation of the section permanently. The length of the core in each section and the core-catcher sample are measured to the nearest centimeter; this information is logged into the shipboard CORELOG database program. Whole-round sections from APC and XCB cores normally are run through the multisensor track (MST). The MST includes the gamma-ray attenuation porosity evaluator (GRAPE) and *P*-wave logger devices, which measure bulk density, porosity, and sonic velocity, and also includes a meter that determines volume magnetic susceptibility. After the core has equilibrated to room temperature (approximately 3 hr), thermal conductivity measurements are performed on relatively soft sediments, and the cores are split.

Cores of soft material are split lengthwise into working and archive halves. The softer cores are split with a wire or saw, depending on the degree of induration. Harder cores are split with a band saw or diamond saw. During Leg 152, the wire-cut cores were split from the bottom to top; thus, investigators should be aware that older material may have been transported up the core on the split face of each section.

The working half of the core is sampled for both shipboard and shore-based laboratory studies. Each extracted sample is logged into the sampling computer database program by the location and the name of the investigator receiving the sample. Records of all removed samples are kept by the curator at ODP. The extracted samples are sealed in plastic vials or bags and labeled. Samples are routinely taken for shipboard PP analysis. These samples subsequently are used for calcium carbonate (coulometric analysis) and organic carbon (CNS elemental analyzer) analyses, and these data are reported in the site chapters.

The archive half is described visually. Smear slides are made from samples taken from the archive half and are supplemented by thin sections taken from the working half. Most archive sections are run through the cryogenic magnetometer. The archive half then is photographed using both black-and-white and color film, a whole core at a time. Close-up photographs (black-and-white) are taken of particular features for illustrations in the summary of each site, as requested by individual scientists.

Both halves of the core then are placed into labeled plastic tubes, sealed, and transferred to cold-storage space aboard the drilling vessel. At the end of Leg 152, the cores were transferred from the ship in refrigerated airfreight containers to cold storage at the Bremen Repository of the Ocean Drilling Program, University of Bremen, Germany.

Igneous and Metamorphic Rocks

Igneous rock cores are handled differently from sedimentary cores. Once on deck, the core-catcher sample is placed at the bottom of the core liner and total core recovery is calculated by shunting the rock pieces together and measuring to the nearest centimeter, this information is logged into the shipboard CORELOG database program. The core then is cut into 1.5-m-long sections and transferred into the laboratory.

The contents of each section are transferred into 1.5-m-long sections of split core liner, where the bottom of oriented pieces (i.e., pieces that clearly could not have rotated top to bottom about a horizontal axis in the liner) are marked with a red wax pencil. This is to ensure that orientation is not lost during the splitting and labeling processes. Important primary features of the cores also are recorded at this time. The core then is split into archive and working halves. A plastic spacer is used to separate individual pieces and/or reconstructed groups of pieces in the core liner. These spacers may represent a substantial interval of no recovery. Each piece is numbered sequentially from the top of each section, beginning with number 1; reconstructed groups of pieces are assigned the same number, but are lettered consecutively. Pieces are labeled only on the outer cylindrical surfaces of the core. If the piece is oriented, an arrow is added to the label pointing to the top of the section. Because pieces are free to turn about a vertical axis during drilling, azimuthal orientation during Leg 152 was possible only by using paleomagnetic or downhole logging data.

When splitting the core, every effort is made to ensure that important features are represented in both halves. The working half is sampled for shipboard PP measurements, magnetic studies, X-ray fluorescence (XRF), X-ray diffraction (XRD), and thin-section studies. Nondestructive physical properties measurements, such as magnetic susceptibility, are performed on the archive half of the core. Where recovery permits, samples are taken from each lithologic unit. Some of these samples are minicores. The archive half is described using the visual core description (VCD) form and is photographed before storage.

The working half of the hard-rock core then is sampled for shipboard laboratory studies. Records of all samples are kept by the curator at ODP. The archive half is described visually, then photographed with both black-and-white and color film, one core at a time. Both halves of the core then are shrink-wrapped in plastic to prevent rock pieces from vibrating out of sequence during transit, placed into labeled plastic tubes, sealed, and transferred to cold-storage space aboard the drilling vessel. As with the other Leg 152 cores, they are housed at the Bremen Repository of the Ocean Drilling Program, University of Bremen, Germany.

Core Descriptions

The core description form (Fig. 3), or barrel sheet, summarizes the data obtained during shipboard analysis of each core. We used the Leg 119 "Explanatory Notes" chapter of the *Initial Reports* volume (Shipboard Scientific Party, 1989a) for a guide because of the similarity of drilling objectives in a heavily glaciated area. The following section summarizes the methods used during Leg 152 to describe sediment cores and the procedures followed to condense the gathered data into summary sheets.

VISUAL CORE DESCRIPTIONS AND THE BARREL SHEET PROGRAM

Sedimentologists during Leg 152 were responsible for visual core descriptions (VCD), smear-slide analyses, and thin-section analyses of all cored sediments and sedimentary rock. Information recorded manually section-by-section on VCD sheets was condensed and entered into the VCD program, thereby producing graphical core description forms. The following is a summary of the use of the VCD program during Leg 152.

The lithology of the recovered material was represented on the computer-generated core description forms by symbols (Fig. 4) representing up to three components in the column titled "Graphic Lithology." Where an interval of sediment or sedimentary rock was a mixture of lithological components, the constituent categories were separated by a solid vertical line, with each category represented by its own symbol. Constituents accounting for <10% of the sediment (or others remaining after the representation of the three most abundant lithologies) were not shown in the "Graphic Lithology" column, but were listed in the "Lithologic Description" section of the core description form. In intervals of thinly interbedded sediments comprising two or more lithologies of different compositions, the constituent categories

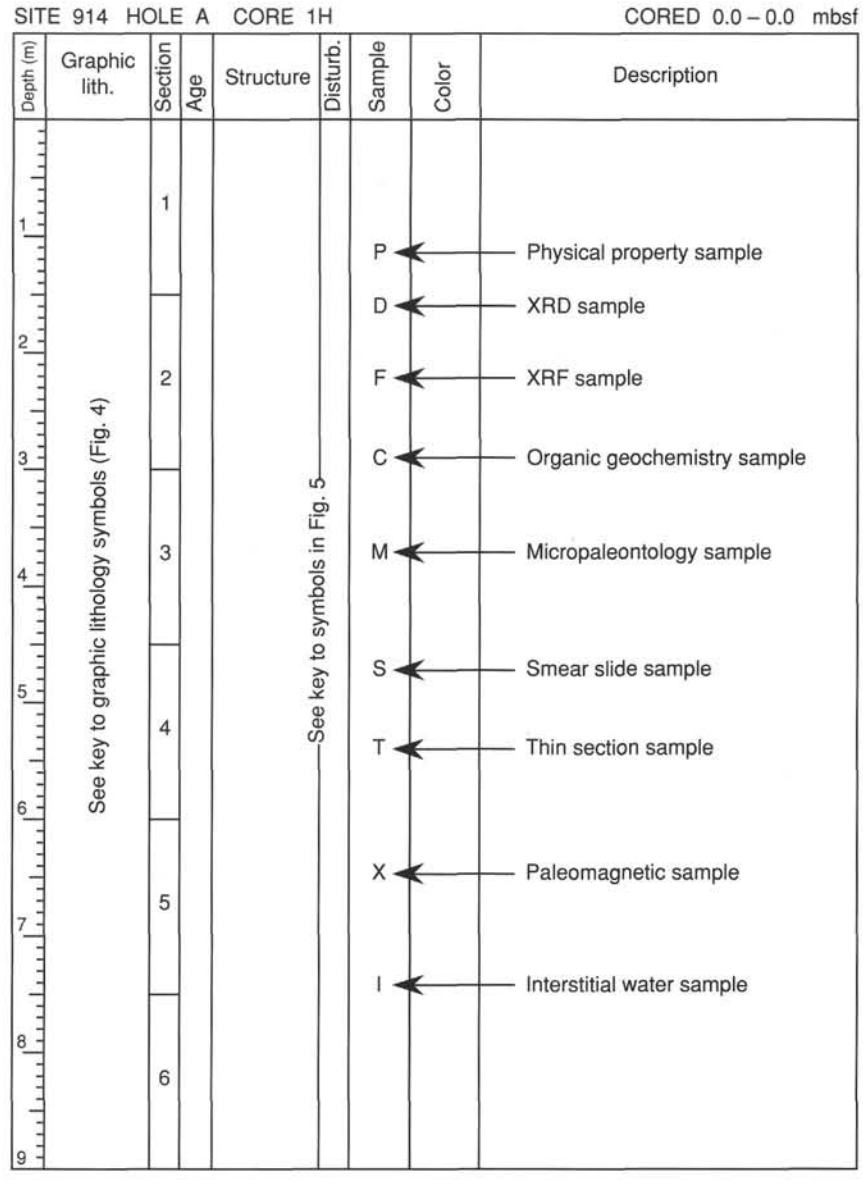

Figure 3. Core description form (barrel sheet) used for samples of sediments and sedimentary rocks.

were separated by a dashed vertical line. Because of the limited scale of the VCD program, the "Graphic Lithology" column shows only the composition of layers or intervals exceeding 20 cm in thickness.

Core Designations

Cores are designated using site, hole, and core number (see "Numbering of Sites, Holes, Cores, Sections, and Samples" section, this chapter). The cored interval is specified in terms of meters below seafloor (mbsf). During Leg 152, these depths were based on drill-pipe measurements, as reported by the ODP operations superintendent.

Age Data

Shipboard paleontologists generally based their age determinations on core-catcher samples, although additional samples were examined when required, such as at suspected age boundaries. The geologic age determined from the paleontological results is shown in the "Age" column (Fig. 3). Detailed information about zonation and terms used to report abundances and preservation appears in the "Biostratigraphy" section (this chapter).

Sediment Disturbance and Rock Fracture

The coring technique, which involved a 25-cm-diameter bit having a 6-cm-diameter core opening, may result in extreme disturbance of the recovered core material and consequently limit observations and interpretation. This disturbance is illustrated in the "Drilling Disturbance" column on the core description form using the symbols in Figure 5. These symbols illustrate the following disturbance categories recognized for soft and firm sediments:

1. Slightly deformed: bedding contacts are slightly bent;
2. Moderately deformed: bedding contacts have undergone extreme bowing;
3. Highly deformed: bedding is completely disturbed; soft sediment may show symmetrical diapir-like structures (flow-in); and
4. Soupy: intervals are water-saturated and have lost all aspects of original bedding.

The following categories are used to describe the degree of fracturing in sedimentary, igneous, and metamorphic rocks (Fig. 5):

1. Slightly fractured: core is broken into pieces which are in place and have very little drilling slurry or breccia.

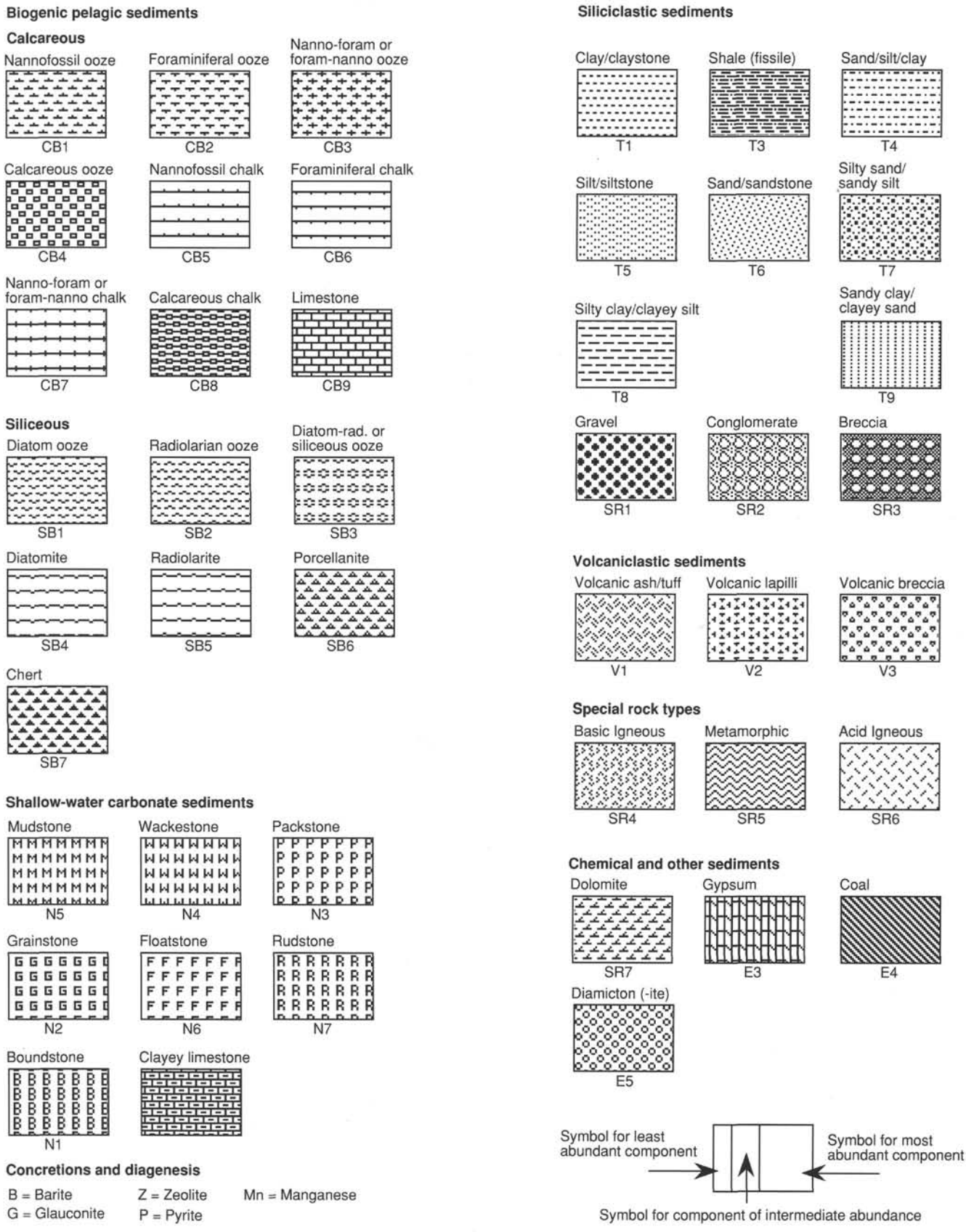

Figure 4. Key to symbols used in "Graphic Lithology" column on the core description form shown in Figure 3.

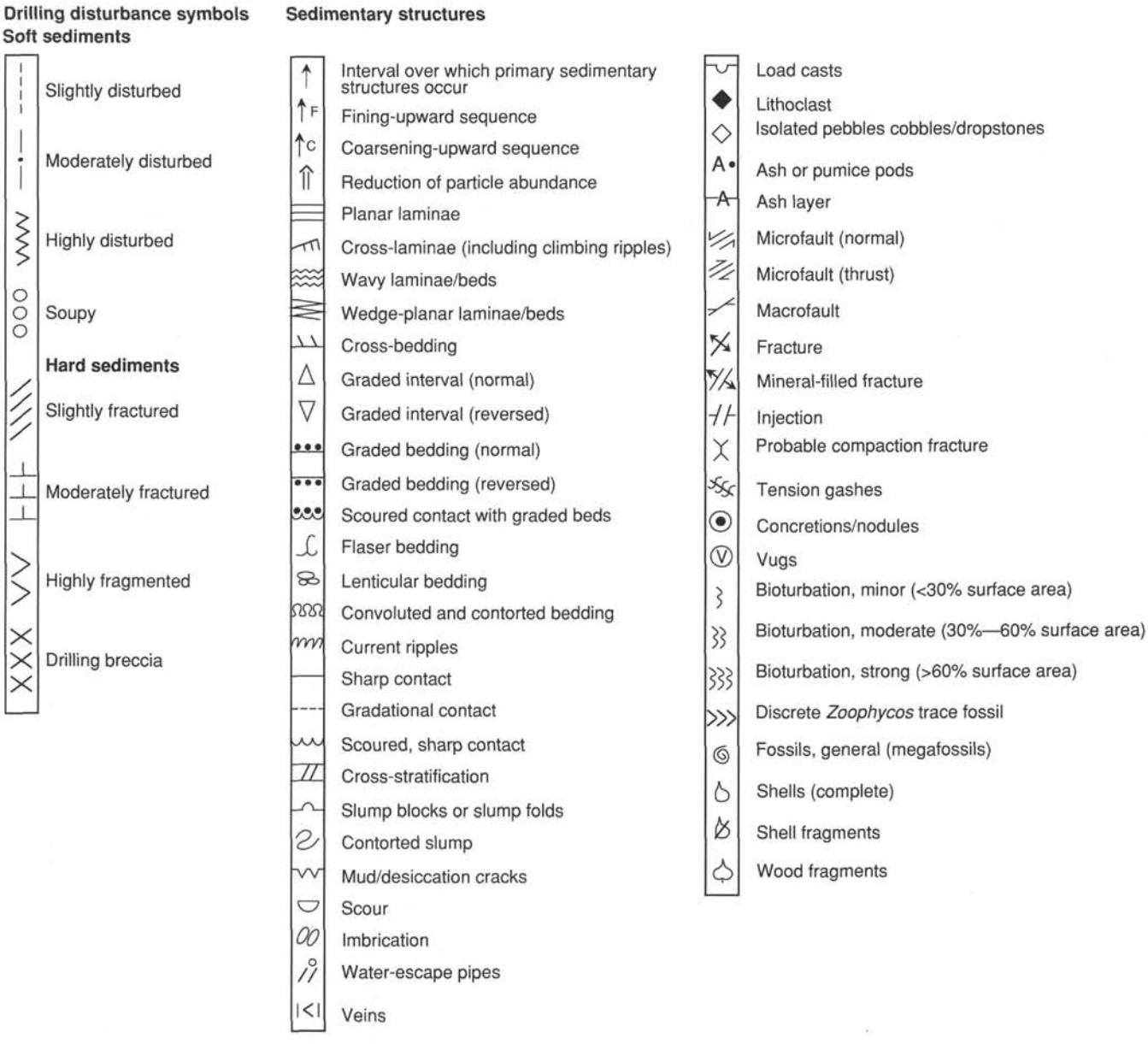

Figure 5. Drilling disturbance symbols used on Leg 152 core description forms. Sedimentary structure symbols for sediments and sedimentary rocks.

2. Moderately fragmented: core pieces are in place or partly displaced, but original orientation is preserved or recognizable; drilling slurry may surround fragments.
3. Highly fragmented: pieces are from interval cored and probably in correct stratigraphic sequence (although they may not represent the entire section), but original orientation is totally lost.
4. Drilling breccia: core pieces have completely lost their original orientation and stratigraphic positions and may be completely mixed with drilling slurry.

Downhole contamination or coring results from loose materials falling from the borehole wall. Most commonly, it occurs at the top of a core as hydrodynamically well-sorted gravel or coarse sand up to 1 m thick, typically having multiple layering and lumps of mixed gravel and soft sediments. A convex conical drilling surface usually lies below the sharp base of the gravel. Isolated pieces of gravel contaminants may occur along the sides of the core liner as far as several meters below the core top.

Sedimentary Structures and Color

Sedimentary structures are indicated in the "Structure" column of the core description form. A key to the sedimentary structural symbols used during Leg 152 is given in Figure 5.

The hue and chroma attributes of color, recorded in the "Color" column of the core description forms, were determined using the Munsell Soil Color Charts (1971) under fluorescent lighting on damp material.

Samples

The location of all samples taken from each core for shipboard analysis is indicated in the "Samples" column on the core description form (Fig. 3).

Lithologic Description

The lithologic description that appears on each core description form consists of two parts: (1) a brief summary of the major litholo-

gies observed in a given core in order of importance, followed by a description of sedimentary structures and features, and (2) a description of minor lithologies observed in the core, their occurrence in the core, and significant features.

A table summarizing smear-slides and thin-section data appears in the Appendix. The section and interval from which the sample was taken are noted, as well as identification as a dominant (D) or minor (M) lithology in the core. The percentage of all identified components (totaling 100%) is listed. These smear slide data are used to classify the recovered material.

Sediment Measurements

Semiquantitative data of low accuracy were compiled on the composition and texture of the sediments by studying smear slides. The smear slides were examined using petrologic microscopes. The percentage of fossil and mineral components, as well as size classes (sand/silt/clay), were estimated visually. Special problems were encountered when estimating clay percentage, in appropriately representing the coarser sand fractions during preparation, and in disaggregating the clay fraction of the semilithified sediments. For Site 918, we used a Lasentec particle size analyzer, which gave repeatable results but probably underestimated the percentage of sand. Inconsistencies among the shipboard sedimentologists when estimating smear-slide compositions contributed to lower accuracies, particularly at the first site.

For routine assignment of sediments to textural classes, grain size was estimated visually from the core material and smear slides. Some samples were selected for grain-size analysis at shore-based laboratories.

SEDIMENT CLASSIFICATION

The sediment classification system used during Leg 152 closely follows that proposed by Mazzullo et al. (1988) for the Ocean Drilling Program. The classification scheme is descriptive, rather than genetic, and is based predominantly on sediment composition and texture. Classification depended entirely on data collected on board the *JOIDES Resolution.* This includes smear-slide analyses for components and grain size, visual core descriptions, and coulometrically determined calcium carbonate contents.

All classification systems present problems, and a few difficulties arose during our studies:

1. Clastic sediments of volcanic provenance (volcaniclastic) are described in the same fashion as siliciclastic sediment, noting the dominant composition of the volcanic grains to avoid premature genetic interpretation.
2. The ODP classification does not adequately address unsorted or poorly sorted siliciclastic sediments, such as those characterized by tills or debris flows. For this type of sediment, we applied the terms diamicton (unlithified) or diamictite (lithified).

Granular Sediments

The following types of grains can be found in granular sediments: (1) pelagic, (2) neritic (calciclastic), (3) siliciclastic, (4) volcaniclastic, and (5) mixed (Fig. 6). Pelagic grains are composed of the organic debris of open-marine, siliceous, and calcareous microfauna and microflora (e.g., radiolarians, nannofossils) and associated organisms. Neritic grains are composed of coarse-grained calcareous (i.e., fossil) debris and fine-grained calcareous grains of nonpelagic origin (e.g., micrite). Siliciclastic grains are composed of mineral and rock fragments derived from igneous, sedimentary, and metamorphic rocks. Volcaniclastic grains are composed of rock fragments, glass, and minerals derived from volcanic sources.

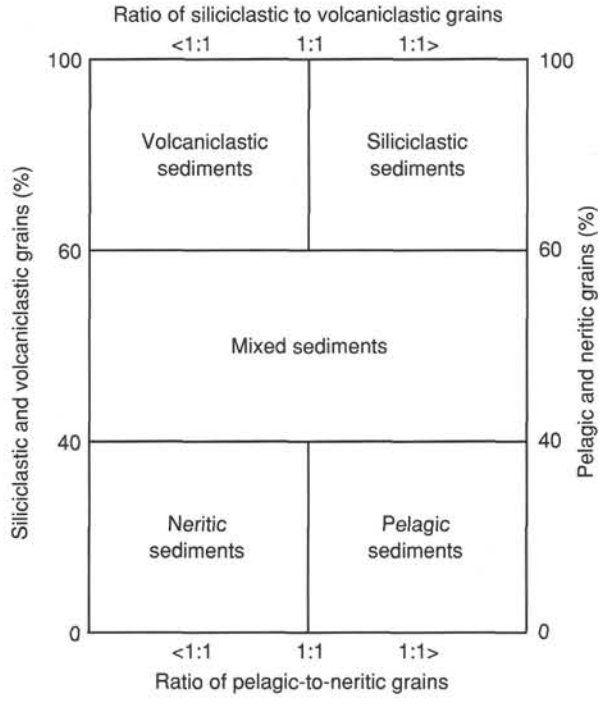

Figure 6. Diagram showing classes of granular sediments.

1. Pelagic sediments are composed of >60% pelagic and neritic grains and <40% siliciclastic and volcaniclastic grains. They also contain a higher proportion of pelagic than neritic grains.
2. Neritic sediments are composed of >60% neritic and pelagic grains and <40% siliciclastic and volcaniclastic grains. They contain a higher proportion of neritic than pelagic grains.
3. Siliciclastic sediments are composed of >60% siliciclastic and volcaniclastic grains and <40% pelagic and neritic grains. They contain a higher proportion of siliciclastic than volcaniclastic grains.
4. Volcaniclastic sediments are composed of >60% siliciclastic and volcaniclastic grains and <40% pelagic and calciclastic grains. They contain a higher proportion of volcaniclastic than siliciclastic grains. This class includes epiclastic sediment (volcanic detritus produced by erosion of volcanic rocks by wind, water, and ice), pyroclastic sediment (products of the degassing of magmas), and hydroclastic sediment (products of granulation by steam explosions and quenching).

The classification of volcaniclastic sediment followed by shipboard scientists during Leg 152 differs somewhat from that proposed by Mazzullo et al. (1988). We followed the siliciclastic textural classification to distinguish the various volcanic sediments (and sedimentary rocks) into volcanic gravel (volcanic conglomerate; grain size greater than 2 mm), volcanic sand (volcanic sandstone; 2 mm–0.0625 mm), volcanic silt (volcanic siltstone, 0.0625 mm–0.0039 mm), and volcanic clay (volcanic claystone, <0.0039 mm). Mixtures of clay and silt are volcanic mud (volcanic mudstone). Sediment modifiers are vitric (glass), crystal (mineral fragments), and lithic. For example, a volcanic sand composed of 45% glass, 35% feldspar crystals and 20% lithic fragments was named a crystal vitric volcanic sand with lithic fragments. Wherever appropriate, comments were added on the core description forms regarding the presumed pyroclastic or epiclastic origin. Furthermore, dispersed volcanic particles (less than 10% from smear-slide observations) have been noted on the core description forms. We use the terms volcanic breccia and volcanic conglomerate for poorly sorted deposits that consist of angular or rounded clasts, respectively, of predominantly volcanic origin, in a fine-grained matrix. When evidence of a primary (pyroclastic) origin was available

for fine-grained sediments, we use the terms lapilli (lapillistone) and ash (tuff), defined by Mazzullo et al. (1988).

5. Mixed sediments are composed of 40% to 60% siliciclastic and volcaniclastic grains and 40% to 60% pelagic and neritic grains.

A granular sediment can be classified by designating a principal name and major and minor modifiers. The principal name of a granular sediment defines its granular-sediment class (Fig. 7); the major and minor modifiers describe the texture, composition, fabric, and/or roundness of the grains.

Glaciogenic Sediments

Glaciogenic sediments pose a particular challenge because of their general paucity in past ODP and DSDP drilling legs and their complex sedimentologic histories. Four general types are described:

1. Distal ice-rafted debris deposited from icebergs that were produced by calving at tidewater glaciers, possibly originating at great distances from the site of deposition;
2. Glacial marine drift produced in areas proximal to floating tidewater glaciers and ice shelves;
3. Subglacial till produced beneath a grounded ice sheet; and
4. Other ice-contact sediments including outwash, subglacial stream deposits, flow-till, glacially tectonized sediments, and so forth.

During Leg 152, sedimentologists followed the classification for siliciclastic sediments (Mazzullo et al., 1988) when describing glaciogenic sediment in the cores, and in addition, we applied the terms diamicton and diamictite for unlithified and lithified, respectively, poorly sorted sediment. Wherever appropriate, comments on the suspected process were made on the core description forms. The following criteria helped us distinguish and interpret glaciogenic sediments:

1. Distal ice-rafted debris: angular dropstones appear in the midst of nonglacial sediments. These sometimes occur in clusters or with other coarse-grained sediments that were dumped when the iceberg tilted or flipped. The nonglacial sequence continues above the dropstone(s).
2. Glacial marine drift: environments adjacent to floating ice termini are complex because sedimentation may occur from calving icebergs, from sediment turbidity flows, and from cold-water plumes that jet from the ice front. The sediment complexities may include numerous dropstones, with the matrix consisting of glacial debris, turbidites, laminated, and bedded sediments. Overall sedimentation rates are very high, measured in centimeters per year.
3. Subglacial till: the weight of glacier ice overriding sediment on the seafloor can produce a massive and compact till that ranges in thickness from centimeters to tens of meters. Some of these tills develop fissility or partings after unloading. Subglacial erosion can produce major unconformities.
4. Other ice-contact sediments: deposits of ice-contact stratified drift, such as subglacial stream deposits, outwash, and flow-till, can form below sea level if the glacier is thick and grounded. A high stream discharge can be maintained, even below sea level.

BIOSTRATIGRAPHY

Preliminary age assignments for Leg 152 sediments have been based on biostratigraphic analysis of calcareous nannofossils and planktonic foraminifers from core-catcher samples. Samples from elsewhere in the cores were examined when more refined age determination was necessary and where time permitted. Benthic foraminifers were used to estimate paleobathymetry. Other microfossil groups (e.g., diatoms, radiolarians, silicoflagellates, and polymorphs) were not studied on board the ship. They will be analyzed and reported by shore-based studies. Sample positions and the abundance, preservation, and chronostratigraphic age or biozone for calcareous nannofossils, planktonic foraminifers, and benthic foraminifers were recorded on barrel sheets for each core. The time scale used is that of Cande and Kent (1992) (Fig. 8).

Calcareous Nannofossils

We referred primarily to the zonation of Okada and Bukry (1980). The zonation of Martini (1971) also is shown in Figure 8 for easy comparison. Wherever possible, we applied nontraditional markers to improve the biostratigraphic resolution.

Smear slides were prepared directly from unprocessed samples and examined with a light microscope at a magnification of about ×1250. The total abundance of calcareous nannofossils for each sample was estimated as follows:

V (very abundant) = >100 specimens per field of view;
A (abundant) = 10–99 specimens per field of view;
C (common) = 1–9 specimen per field of view;
F (few) = 1 specimen per 2–10 fields of view; and
R (rare) = 1 specimen per 11–200 fields of view.

Abundances of individual species were estimated for each sample, with the following approximate definitions:

V (very abundant) = >10 specimens per field of view;
A (abundant) = 1–10 specimens per field of view;
C (common) = 1 specimen per 2–10 fields of view;
F (few) = 1 specimen per 11–50 fields of view; and
R (rare) = 1 specimen per 51–200 fields of view.

The qualitative evaluation of the preservation of calcareous nannofossils was recorded as:

G (good) = specimens exhibit little evidence of dissolution and/or overgrowth;
M (moderate) = specimens exhibit moderate dissolution and/or overgrowth, and a significant proportion (up to 20%) of the specimens cannot be identified to species with absolute certainty; and
P (poor) = specimens exhibit severe dissolution and/or overgrowth, and more than 20% of the specimens cannot be identified at the species level.

Planktonic Foraminifers

The low and middle latitude zonations of Berggren and Miller (1988) and of Blow (1969, 1979), modified by Kennett and Srinivasan (1983), were tentatively applied, whenever possible, to Paleogene and Neogene assemblages, respectively. If a general absence of any marker species prevented the application of such zonal schemes, the zonations of Berggren (1972) and Weaver and Clement (1987), proposed for the North Atlantic, and that of Spiegler and Jansen (1989), based on the neogloboquadrinids proposed for the Norwegian Sea, were applied to Paleogene to Quaternary assemblages. Moreover, compositions of assemblages and additional bioevents were taken into account to improve the stratigraphic resolution (Fig. 9).

Samples of about 10 cm^3 taken from the core-catchers and/or elsewhere from the cores were soaked in diluted hydrogen peroxide and then washed under running water through 40-µm-mesh sieves. The 40-µm-mesh sieve was used to retain small-sized specimens and/or species, such as pseudohastigerinids, tenuitellids, and chiloguembelinids. In case of abundant residues, the 40- to 150-µm and >250-µm sieves were used, and three fractions were obtained for paleoclimatic investigations (Spezzaferri, 1992). The obtained fractions then were dried on a hot plate and studied under a binocular microscope.

The abundance of single species within the assemblages in the residues was recorded as:

VA = very abundant (>60% of the total fauna);
A = abundant (40%–60%);

F = frequent (20%–40%);
C = common (5%–20%); and
R = rare (<5%).

Preservation includes the effect of diagenesis, abrasion, recrystallization, encrustation, and/or dissolution of planktonic foraminifer tests. The degree of preservation of tests has been expressed as follows:

G = good (no or low dissolution effects are observable);
M = moderate (minor but common dissolution, specimens are still recognizable); and
P = poor (strong dissolution affects the assemblages, species identification very difficult or impossible).

Benthic Foraminifers

Assemblages of benthic foraminifers are mainly governed by water depth, water mass, nutrient supply, and nature of substrata (e.g., Murray, 1984; Osterman and Qvale, 1989). Preliminary analyses of benthic foraminifers on board the ship were used to estimate paleowater depths. The following terms were used to characterize water-depth ranges:

sublittoral = 0–200 m;
upper bathyal = 200–500 m;
middle bathyal = 500–1500 m;
lower bathyal = 1500–3000 m; and
abyssal = >3000 m.

Preparation of benthic foraminifers followed standard techniques. Briefly, samples were soaked in diluted hydrogen peroxide, washed over a sieve having an opening of 63 µm, dried, and examined under a binocular microscope. For calculating abundances of benthic foraminifers, the samples were split first if they were rich in benthic foraminifers. For samples having low abundances of benthic foraminifers, all benthic foraminifers were picked. The abundances of individual species were recorded as:

A = abundant (>27% of the total assemblage);
C = common (9%–27%);
F = few (3%–9%); and
R = rare (<3%).

The state of preservation was recorded as:

G = good (little or no fragmentation, overgrowth, and/or dissolution);
M = moderate (some signs of fragmentation, overgrowth, and/or dissolution); and
P = poor (severe fragmentation, heavy overgrowth, and/or dissolution).

PALEOMAGNETISM

Paleomagnetic studies performed on the *JOIDES Resolution* during Leg 152 included analysis of the natural remanent magnetization (NRM), magnetic susceptibility, isothermal remanent magnetization (IRM), and anhysteretic remanent magnetization (ARM). The bulk of the NRM and susceptibility data was obtained from whole-core analysis of the archive core sections and whole-core rounds, respectively. Discrete specimens were used for the magnetostratigraphic and mineralogical investigations to supplement the whole-core remanence and susceptibility studies.

Laboratory Instruments

The remanence of all archive-half sections was measured using a 2G Enterprises whole-core cryogenic (WCC) magnetometer, which has an in-line three-axis alternating field (AF) demagnetization system capable of generating fields of 30 mT. The demagnetizing coils used in this system are enclosed in a µ-metal shield that attenuates the ambient field to ~100 nT. The µ-metal shields were de-Gaussed if the ambient field within the demagnetizing region exceeded 100 nT. Each

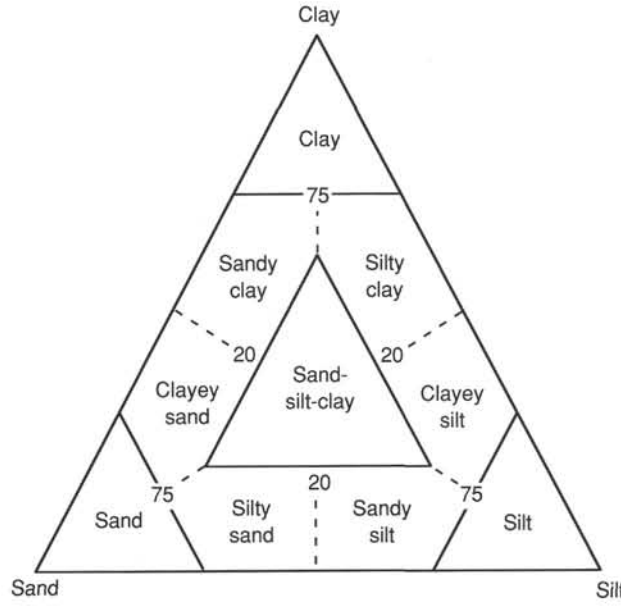

Figure 7. Ternary diagram showing principal names for siliciclastic sediments (from Shephard, 1954).

of the sense coils in the WCC have slightly different response curves, but effectively, they measure the signal over the ~20-cm length of core. This length corresponds to a ~380-cm^3 volume of material that contributes to the remanence measured at any point in the core. Such a volume enables weakly magnetized rocks and sediments to be measured accurately despite the background noise of the magnetometer. The WCC system is controlled by a PC-AT-compatible computer running a Quick Basic program.

Discrete samples collected from the working half of the core were measured using either the WCC magnetometer, in discrete sample mode, or a "Molspin" spinner magnetometer (MSM). The MSM was controlled by a Macintosh IIci, using software developed by Dave Schneider Ltd. (installed on *JOIDES Resolution* for Leg 138).

Specimens processed on the MSM were demagnetized using a Schonstedt stationary sample AF demagnetizer (Model GSD-1) to peak field of 100 mT. No thermal demagnetization was performed.

The magnetic susceptibility of whole cores was measured with a Bartington Instruments magnetic susceptibility meter (Model MS1, adapted with a MS1/CX 80 mm whole-core sensor loop set at 0.465 kHz), mounted with the GRAPE and *P*-wave logger on the MST. The full width of the impulse response peak at half maximum is less than 5 cm. The susceptibility of discrete specimens was measured on board the ship with a sensor unit (type MS1B) attached to the Bartington susceptibility meter.

For Leg 152, an Analytical Services Company (ASC) Model IM-10 impulse magnetizer was used for IRM studies. The magnetizer was used to apply pulsed fields of between 20 and 1200 mT to discrete specimens.

Sampling Technique

Core Orientation

Core orientation of the APC cores was attempted on a case-by-case basis by using a Tensor multishot tool that is mounted onto a nonmagnetic sinker bar. At the bottom of the hole, the core barrel was allowed to rest for sufficient time (2–8 min) to permit an accurate reading of the magnetic and gravity sensors. The Tensor tool consists of three mutually perpendicular magnetic sensors and two perpendicular gravity sensors. The information from both sets of sensors allows one to measure the azimuth and dip of the hole as well as the azimuth of the APC core

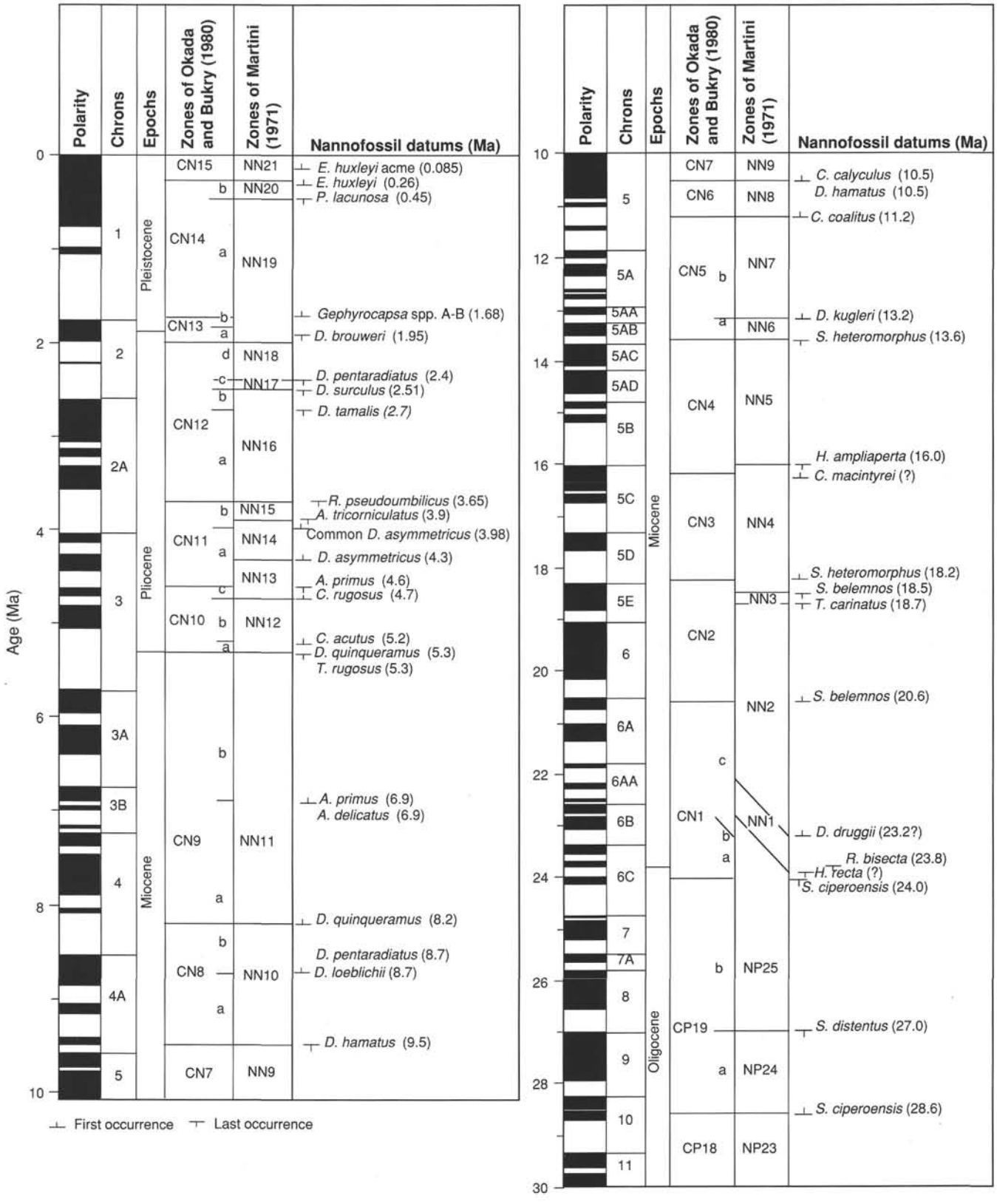

Figure 8. Correlation of nannofossil datums and zones/subzones with the geomagnetic polarity time scale of Cande and Kent (1992).

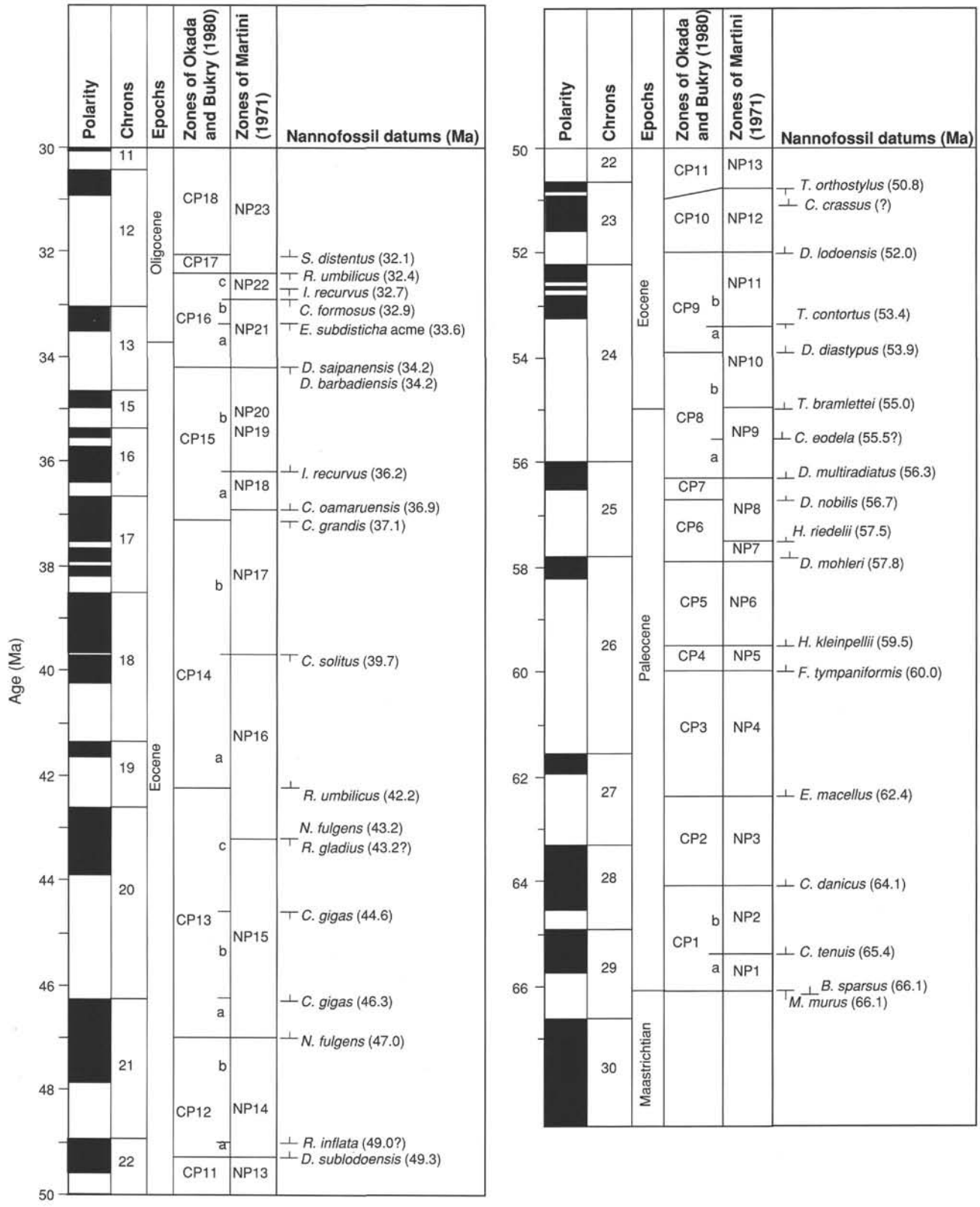

Figure 8 (continued).

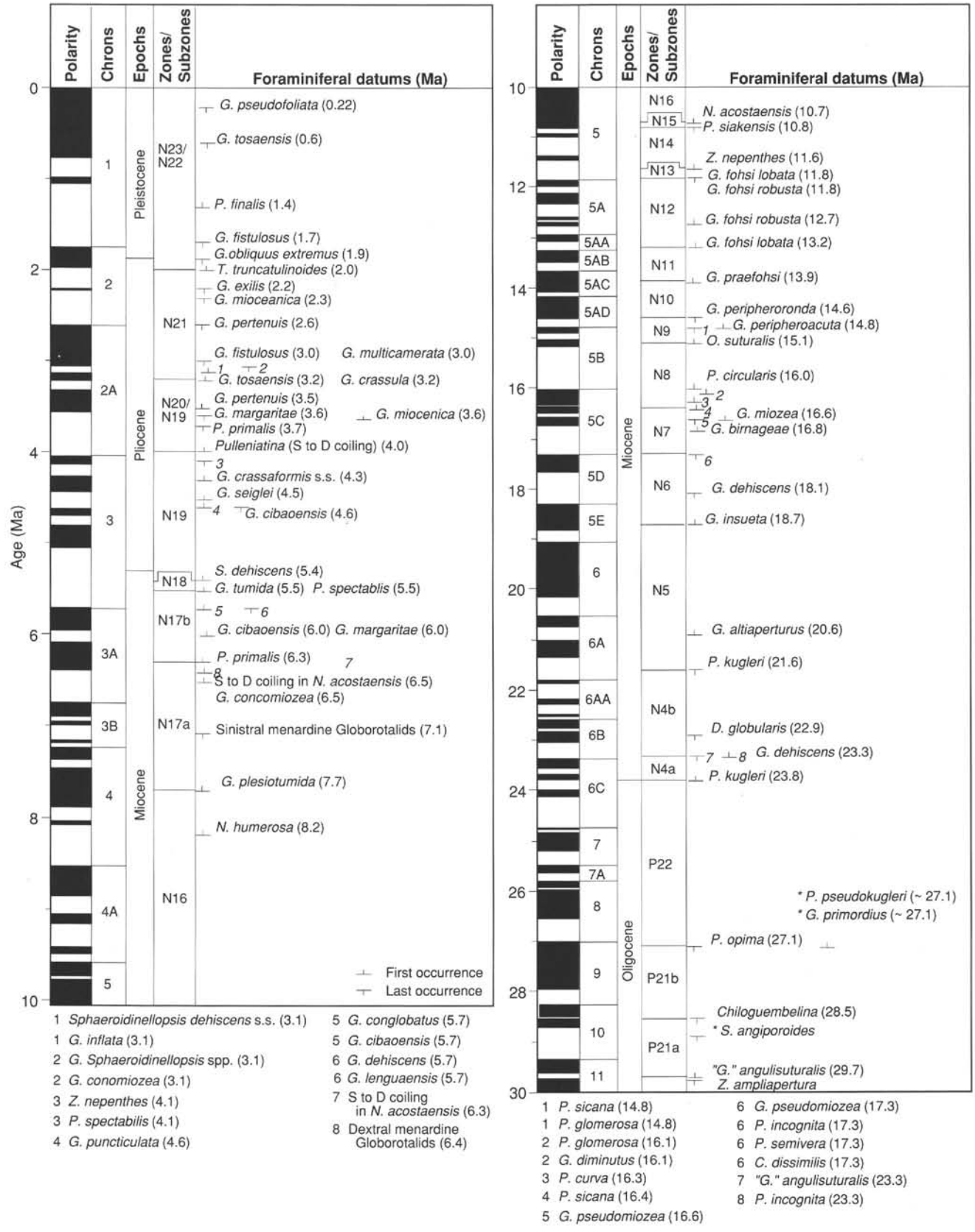

Figure 9. Correlation of planktonic foraminifer datums and zones with the geomagnetic polarity time scale of Cande and Kent (1992). Planktonic foraminifers zonations used are those of Berggren and Miller (1992). Planktonic foraminifer zonations used are those of Berggren and Miller (1988) for Paleogene and Blow (1969, 1979), modified by Kennett and Srinivasan (1983), for Neogene. Ranges of *Subbotina angiporoides, Paragloborotalia pseudokugleri*, and *G. primordius* are from Spezzaferri (1992).

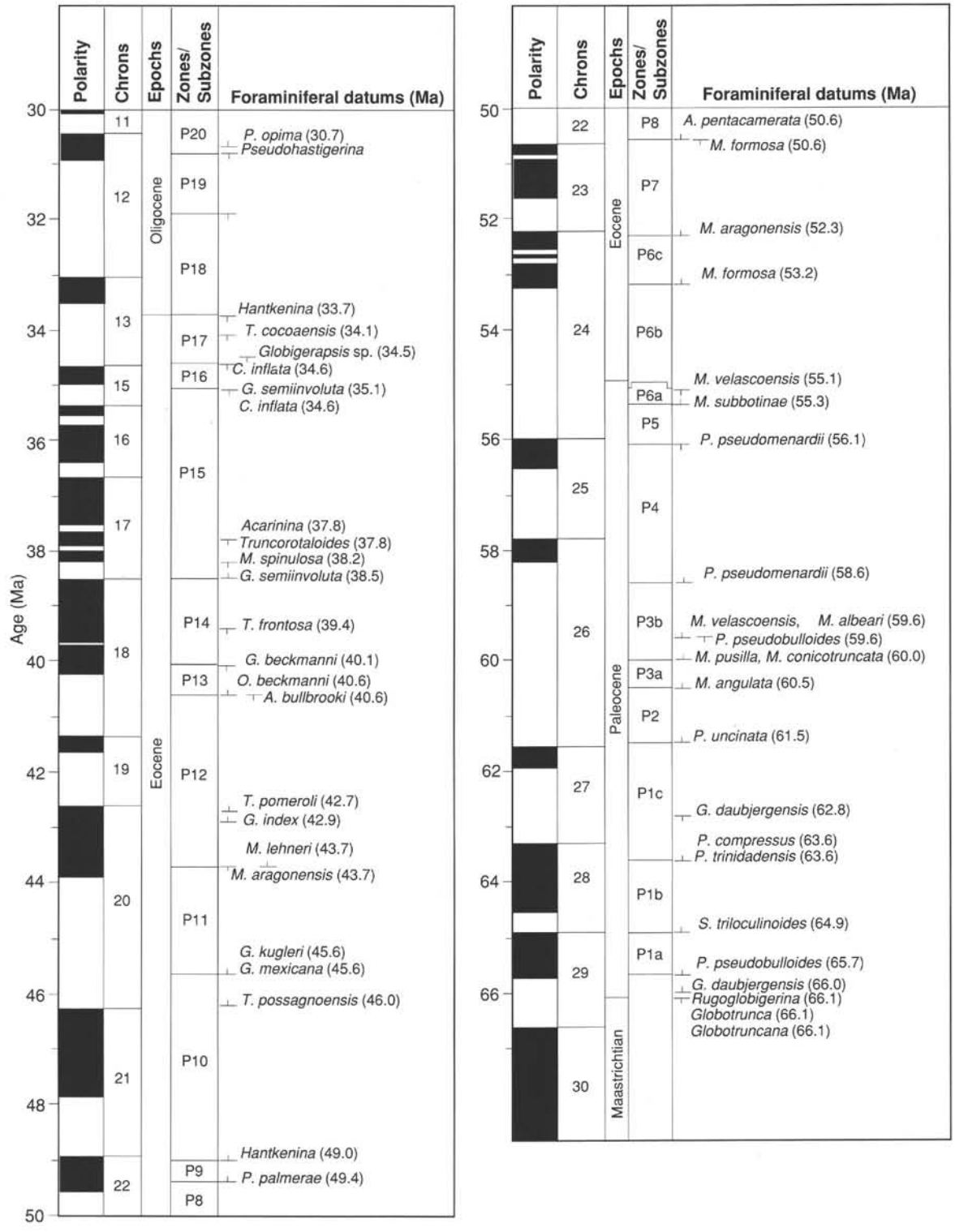

Figure 9 (continued).

double orientation line. The Tensor tool was used to collect oriented cores for investigating secular variation within Quaternary sediments.

Discrete Sampling

Discrete samples in soft sediment were taken using oriented standard plastic boxes (6 cm^3). To minimize sediment deformation, the core was cut using a scalpel before pressing the plastic sampling boxes into the sediment. Minicores (12.9 cm^3) were drilled from lithified sedimentary and igneous rocks using a water-cooled nonmagnetic drill bit attached to the standard drill press.

Magnetic Experiments

Remanent Magnetization Measurements

Remanence measurements of sediments were performed by passing continuous archive-half core sections through the WCC. The ODP

core orientation scheme arbitrarily designates the positive *X*-axis direction as the horizontal (in-situ) line radiating from the center of the core through the space between a double line scribed lengthwise on the working half of each core liner.

Two or three AF demagnetization levels (up to 30 mT) were performed on each archive-whole section to isolate characteristic magnetizations. More detailed demagnetization analysis was performed using discrete specimens to confirm the presence, or otherwise, of magnetozones identified from the WCC measurements.

Magnetic Direction Determination

Both Zijderveld (1967) plots and equal-area stereographic projections were used to determine the stability of remanence of levels within the archive cores and for the discrete specimens.

Magnetostratigraphy

Magnetozones were defined on the basis of at least two successive depths of the same polarity, and the boundary between two successive magnetozones was defined by the depth at which the interpolated inclination record crossed zero inclination. The ultimate time resolution of the paleomagnetic record depends on sediment accumulation rates and the resolution of the pass-through measurements, which are limited to approximately 10 cm by the coil geometry. For shipboard measurements, the measurement interval was generally 10 cm, but was sometimes reduced to 5 cm, when the reversal rate increased or when short events were suspected.

A subset of the shipboard samples were AF-demagnetized in the GSD-1 to evaluate the effectiveness of the pass-through demagnetization routine for isolating a characteristic magnetization.

Where AF demagnetization isolated a consistent record of geomagnetic polarity, we offer in the site chapters an interpretation of the magnetic polarity stratigraphy of the recovered core. Magnetochron assignments were established using nannofossil and planktonic foraminiferal data with the magnetostratigraphic and biostratigraphic scales of Berggren, Kent, and Flynn (1985) and Berggren, Kent, and Van Couvering (1985). The geomagnetic polarity time scale of Cande and Kent (1992) provides the chronostratigraphic frame (see "Biostratigraphy" section, this chapter). For the upper part of the time scale (roughly Pliocene–Pleistocene), we used the traditional proper or place names to refer to various chrons and subchrons. For older sediments, we adopted the chronozone-labeling notation proposed by Cande and Kent (1992, p. 13948).

The magnetic record preserved in the sediments and rocks recovered during Leg 152 appears to include short geomagnetic features. The mechanism generating these features is not yet fully understood, but we recognized their potential for providing additional stratigraphic markers with which to subdivide and correlate the geological succession. Specific events are discussed in the "Paleomagnetism" sections (this volume) for each of the sites.

Low-field Susceptibility

Whole-core susceptibility measurements are relatively rapid to make, are nondestructive, and provide an indication of the amount of magnetizable (ferrimagnetic and paramagnetic) material in the sediment. Whole-core volume magnetic susceptibility was measured with the automated MST. Measurements were performed at the low sensitivity range (1.0) and in the SI mode, usually every 2 cm. The susceptibility response is a function of the mineralogy as well as the shape and volume of the magnetic particles within the rocks. Because magnetic susceptibility is slightly temperature-dependent, the cores were permitted to equilibrate thermally prior to analysis. The general trend of the susceptibility data curve was used to characterize the magnetic material contained within the cored sediments as well as subtle environmental and geological changes within the sediments.

Volume magnetic susceptibility also was measured on discrete samples with the Bartington susceptibility meter.

Additional Magnetic Measurements

The measurements of natural remanence and susceptibility generally were supplemented by analysis of ARM and IRM. These experiments permitted a preliminary estimate of the magnetic mineralogy of sediments and volcanic rocks.

ARM values were measured using the Schonstedt AF demagnetizer and DTECH, Inc. double core device. The instrument enables one to apply a steady, unidirectional field of 0.1 mT during each AF step. Discrete samples were subjected to progressive stepwise ARM (to a peak field of 100 mT). The ARM was measured between steps using the MSM.

IRM acquisition experiments were performed using the ASC scientific impulse magnetometer. Samples were subjected to a stepwise IRM along the *X* axis to peak fields of 1.2 T. The resulting IRM was also measured between steps using the MSM.

IGNEOUS PETROLOGY

Core Curation and Shipboard Sampling

To preserve important features and structures, core sections containing igneous rocks were examined prior to splitting. During core handling and splitting, core orientation was preserved by marking the base of individual pieces with a red chinagraph pencil. Each piece was numbered sequentially from the top of each core section and was labeled at the top surface. Pieces that could be fitted together were assigned the same number and were lettered consecutively (e.g., 1A, 1B, and 1C). Plastic spacers were placed between pieces having different numbers. The presence of a spacer, therefore, may represent a substantial interval of no recovery. After the vertical core orientation was noted, the pieces were split with a diamond-impregnated saw into archive and working halves, with care taken to ensure division of key features.

Nondestructive physical-properties measurements, such as magnetic susceptibility and natural gamma-ray emission, were taken on the core before it was split. After the core was split, the working half was sampled for shipboard physical properties, magnetic studies, XRF, XRD, and thin-section studies. Samples were taken from most of the lithological units for thin-section studies and XRF major- and trace-element analysis. The archive half was described on the visual core description form and was photographed before storage.

Visual Core Descriptions

Visual core description forms were used when documenting the igneous rock cores (see "Cores" Section, this volume). The left column on the form is a graphical representation of the archive half. A horizontal line across the entire width of the column denotes a plastic spacer. Oriented pieces are indicated on the form by an upward-pointing arrow to the right of the piece. Shipboard samples and studies are indicated in the column headed "Shipboard Studies" with the following notation: D = XRD analysis; F = XRF analysis; T = petrographic thin section; P = physical-properties analysis; and M = palaeomagnetic analysis.

The core was subdivided into consecutively numbered lithologic units (mostly representing single lava flows) on the basis of changes in color, structure, grain size, and mineral occurrence and abundance. Some units were divided into subunits (A, B, etc.) because of uncertainty about the number of individual flows involved. Further, to preserve the continuity of numbering of the igneous units, intercalated sediment horizons were designated as "A" and the underlying volcanic rock as "B" within the same unit. Likewise, breccia or mylonite zones within units led to subdivision into, for example, A, B (brecciated zone), and C subunits.

The visual core descriptions were entered into the computer database HARVI. This database is divided into separate compartments for fine-grained and coarse-grained rocks. All the volcanic rocks were entered into the fine-grained compartment. Each record is checked by the database program for consistency and completeness and is subsequently printed in a format that can be directly merged with the visual core description sheet to form a complete core section description (see "Cores" Section, this volume). Separate HARVI records were made for each core section, and if more than one lithological unit was present in a section, separate records were made for each unit. Each HARVI record comprises the following information.

1. The leg, site and hole, core number and core type, and section number.
2. The unit number (consecutively downhole), the rock name (see below) and the number of pieces.
3. Contact relationships with neighboring lithologic units.
4. Phenocrysts: number of mineral phases visible with a hand lens or under a binocular microscope and their distribution within the unit, and for each phase its abundance (vol%), size range (mm), shape, degree of alteration, and further comments if appropriate.
5. Groundmass texture and grain size: glassy, aphanitic, fine-grained (<1 mm), medium-grained (1–5 mm), or coarse-grained (>5 mm). Grain size changes within units also were noted.
6. Vesicles: abundance, distribution, size, shape, and mineral linings and fillings.
7. Color name and code (for the dry rock), according to the Munsell Color Charts.
8. The rock structure: whether the unit is massive, flow-banded, flow-brecciated, scoriaceous, pillowed, hyaloclastic, or tuffaceous.
9. Alteration: alteration was graded as fresh (<5%), slight (5%–10%), moderate (10%–40%), strong (40%–90%), and complete (90%–100%). Changes of alteration through a section or a unit also were noted.
10. The presence of veins and fractures, including their abundance, width, mineral linings and fillings, and, where possible, their orientation.
11. Additional comments, including notes on the variability of the unit.

The rocks were described as aphyric when no phenocrysts were visible with a hand lens or under a binocular microscope. The name "aphyric olivine basalt" was applied when olivine or its alteration products was considered to be present in the groundmass, whereas "aphyric basalt" was applied when little or no olivine was seen in the groundmass. Porphyritic rocks were named by phenocryst type, using mineral names in order of decreasing abundance. "Picrite" was defined as a rock having at least 15% olivine phenocrysts. The rock names were assigned initially on the basis of hand-specimen observation and later were checked with the thin sections, especially concerning the occurrence of olivine in the groundmass.

Visual core descriptions of igneous rocks are given in the "Cores" Section (this volume), and descriptions of each rock unit also are available from the HARVI database.

Thin-section Descriptions

Thin sections of most of the lithological units were examined to complement and refine the hand-specimen observations. The percentages of various components present in the thin sections either were estimated visually or were determined by counting 500 points using an automatically advancing stage with an attached counter. The percentages and textural description of individual phases were reported in the database HRTHIN. All textural terms used were defined in MacKenzie et al. (1982). The same terminology was used for thin-section descriptions as was used for the visual core descriptions. For some porphyritic basalts, the thin section and visual core descriptions differ slightly, typically because small plagioclase laths in a rock with seriate texture are only visible in thin section. Thus, a rock visually described as olivine-plagioclase-phyric may be plagioclase-olivine-phyric, according to the thin-section description. Because not all units were examined in thin section, this discrepancy has been accepted and retained to maintain consistency of the visual records. Thin-section descriptions of igneous rocks are given in the "Thin-section Descriptions" Section (this volume) and are also available from the HRTHIN database.

XRF Analysis

Samples representative of most of the lithological units were selected for shipboard XRF analysis. Large pieces were reduced to a diameter of less than 1 cm by crushing between two disks of Delrin plastic in a hydraulic press. The sample was then ground for approximately 5 min in a Spex 8510 shatterbox with a tungsten carbide barrel.

The possibility of contamination of the samples with Nb during grinding was investigated by A.D. Saunders and N.G. Marsh in the Department of Geology at Leicester University before the start of Leg 152. Separate aliquots of four rock samples (three basalt and one gabbro) known to have low Nb contents were ground using both the shipboard tungsten carbide barrel and an agate-lined mill. Both sets of powders were then analyzed for Nb (and other elements) using an ARL XRF spectrometer similar to that on board the ship. No Nb contamination was detected within the precision limits. The results are given in Table 1.

A fully automated wavelength-dispersive ARL8420 XRF system equipped with a 3-kW generator and a Rh-anode X-ray tube was used to determine the major- and trace-element abundances in the samples. Analytical conditions used are given in Table 2. The spectrometer was calibrated using a suite of well-analyzed reference standards (AGV-1, AII-92, BE-N, BHVO-1, BIR-1, BR, DR-N, G-2, GH, JB2, JB3, JGB1, K1919, RGM-1, UB-N). The values recommended by Govindaraju (1989) were used for all elements, except for Zr and Nb. A subset of the standards, with concentrations recommended by Jochum et al. (1990), was used for these two elements. Precision estimates, based on replicate shipboard analyses of the USGS reference standard BIR-1, are given in Tables 3 (major elements) and 4 (trace elements).

Major-element analyses were performed on fused lithium borate glass disks doped with lanthanum oxide as a heavy absorber (Norrish and Hutton, 1969). These disks were prepared from 500 mg of rock powder that had been ignited for 2 hr at about 1100°C, mixed with 6.000 g of dry flux that consisted of 80% lithium tetraborate and 20% lanthanum oxide. This mixture was then melted in air at 1150°C in a Pt-Au crucible for about 4 min with constant agitation to ensure thorough mixing and then poured into a Pt-Au mold. The 12:1 flux:sample ratio and the use of the heavy absorber make matrix effects insignificant over the normal range of igneous rock compositions. Hence, the relationship between X-ray intensity and element concentration is linear.

Trace elements were determined on pressed-powder pellets. These were made by mixing 7 g of rock powder with 30 drops of a solution of Chemplex polymer in methylene chloride (100 mg/cm^3) and then pressing the mixture into an aluminum cap under a load of 8 tons. A pellet made with 5 g of basalt powder should be infinitely thick at the shortest wavelengths used in the analysis. X-ray intensities were corrected for line-overlap and inter-element absorption effects. The latter corrections were based on the relationship between mass absorption coefficient and the intensity of the RhKα Compton scatter line (Reynolds, 1963, 1967; Walker, 1973). Duplicate analyses of Sample 152-917A-58R-2, 33–37 cm, indicate that reproducibility of all elements is better than 5% except for Nb, Ce, and Rb, which are reproducible to 20%, 22%, and 15%, respectively. These elements are present in low concentrations in many of the samples. Two sets of analyses of separate samples from the same unit differ by only slightly more than the precision indicated by the replicate analyses, suggesting that the 15- to 20-cm^3 sample volume selected for XRF analysis was sufficient to be representative of the sample.

Table 1. Comparison of trace-element contents of basic rock samples ground in an agate mill and in the shipboard tungsten carbide barrel.

	Basalt 1		Basalt 2		Basalt 3		Gabbro 1	
Element	Agate	WC	Agate	WC	Agate	WC	Agate	WC
Nb	5.6	5.8	5.9	5.9	8.8	8.8	1.3	0.9
Zr	117.5	115.7	114.4	116.2	164.0	163.6	23.4	20.0
Y	33.4	33.3	31.3	31.0	33.6	33.6	10.7	9.9
Sr	245.0	249.3	270.0	266.2	317.5	316.1	215.4	221.2
Rb	36.3	37.7	9.9	10.3	27.2	28.0	3.2	2.3
Zn	91.3	91.7	91.1	94.7	91.2	90.4	31.4	30.5
Ba	171.9	178.4	168.1	165.5	324.6	314.7	66.7	70.9

Notes: Element abundances were determined on powder pellets at the University of Leicester (U.K.) Analytical conditions are given in Pickering et al. (1993). Trace-element contents in ppm; WC = shipboard tungsten carbide barrel.

Table 2. Leg 152 XRF analytical conditions.

					Peak	Background	Total count time	
Element	Line	Crystal	Detector	Collimator	angle (deg.)	offset (deg.)	Peak (s)	Background (s)
SiO_2	Kα	PET (002)	FPC	Coarse	109.21	0	40	0
TiO_2	Kα	LiF (200)	FPC	Fine	86.11	0	40	0
Al_2O_3	Kα	PET (002)	FPC	Coarse	145.18	0	100	0
Fe_2O_3*	Kα	LiF (200)	FPC	Fine	57.47	0	40	0
MnO	Kα	LiF (200)	FPC	Fine	62.93	0	100	0
MgO	Kα	TLAP	FPC	Coarse	45.17	±0.80	150	300
CaO	Kα	LiF (200)	FPC	Coarse	113.12	0	40	0
Na_2O	Kα	TLAP	FPC	Coarse	55.10	−1.20	150	150
K_2O	Kα	LiF (200)	FPC	Coarse	136.69	0	100	0
P_2O_5	Kα	Ge (111)	FPC	Coarse	141.09	0	100	0
Nb	Kα	LiF (200)	Scint	Fine	21.40	−0.35	200	200
Zr	Kα	LiF (200)	Scint	Fine	22.55	−0.35	100	100
Y	Kα	LiF (200)	Scint	Fine	23.80	−0.40	100	100
Sr	Kα	LiF (200)	Scint	Fine	25.15	−0.40	100	100
Rb	Kα	LiF (200)	Scint	Fine	26.62	−0.60	100	100
Zn	Kα	LiF (200)	Scint	Coarse	41.81	−0.40	100	100
Cu	Kα	LiF (200)	Scint	Fine	45.03	−0.40	100	100
Ni	Kα	LiF (200)	Scint	Coarse	48.67	−0.60	100	100
Cr	Kα	LiF (200)	FPC	Fine	69.35	−0.50	100	100
TiO_2	Kα	LiF (200)	FPC	Fine	86.11	+0.50	40	40
V	Kα	LiF (220)	FPC	Fine	123.06	−0.50	100	100
Ce	Lα	LiF (220)	FPC	Coarse	128.13	1.50	100	100
Ba	Lβ	LiF (220)	FPC	Coarse	128.78	1.50	100	100

Notes: *Total Fe as Fe_2O_3. FPC = Flow proportional counter using P10 gas. Scint = NaI scintillation counter. Trace elements analyzed under vacuum using goniometer 2 at generator settings of 60 kV and 50mA. Major elements analyzed under vacuum using goniometer 2 (1 for Na and Mg) at generator settings of 30 kV and 80 mA.

ORGANIC GEOCHEMISTRY

The shipboard organic geochemical investigations for Leg 152 include (1) real-time monitoring of the volatile hydrocarbons, as required by ODP safety considerations; (2) measurement of the inorganic carbon concentration to determine the amount of carbonate in the sediments; (3) elemental analysis of nitrogen, total carbon, and sulfur; and (4) determination of free hydrocarbons, pyrolyzable hydrocarbons, and maturity of organic matter. A more detailed description of the analytical procedures is given in Emeis and Kvenvolden (1986) and in the "Explanatory Notes" chapter of Leg 146 *Initial Reports* volume.

Hydrocarbon Gases

As required by safety and pollution prevention considerations, the concentrations of the low-molecular-weight hydrocarbons methane (C_1), ethane (C_2), and propane (C_3) are monitored in the sediment cores at intervals of approximately 10 m. A 5-cm^3 sample is removed from the end of the core immediately after its arrival on deck and is placed in a glass vial that is sealed and then heated to 70°C for at least 30 min (Kvenvolden and McDonald, 1986). Whenever gas pockets or expansion voids are observed, vacutainer samples are taken as well.

The gas samples obtained are injected into a Hach-Carle AGC series 100, Model 211 gas chromatograph equipped with a flame ionization detector and a 6 ft × 1/8 in. steel column packed with Porapak N:Q (80%/20%). The gas chromatograph has a detection limit for methane of 0.1 ppm. Details of this method and the complete configuration of the instrument are given in the "Explanatory Notes" chapter of the Leg 112 *Initial Reports* volume (Suess, von Huene, et al., 1988).

Inorganic Carbon

Inorganic carbon is determined using a Coulometrics 5011 carbon dioxide coulometer equipped with a System 140 carbonate carbon analyzer. Approximately 70 mg of freeze-dried, ground, and weighed sediment is used for each measurement.

The percentage of carbonate then is calculated from the inorganic carbon content, assuming that all the carbonate occurs as calcium carbonate, as follows:

$$CaCO_3 = IC \text{ (inorganic carbon)} \cdot 8.33.$$

No corrections are made for other carbonate minerals, such as siderite or dolomite.

Elemental Analysis

The nitrogen, total carbon (TC), and sulfur content of the sediment samples are determined by a Carlo Erba Model NA 1500 NCS analyzer. In the NCS analyzer, freeze-dried and ground samples are combusted at 1000°C in an oxygen stream. Nitrogen oxides are reduced to N_2, and the mixture of CO_2, SO_2, and N_2 is separated by

Table 3. Major-element analytical precision.

Element	Published values	Mean (n = 15)	1 σ
SiO_2	48.04	47.322	0.200
TiO_2	0.96	0.965	0.011
Al_2O_3	15.53	15.320	0.060
Fe_2O_3	11.34	11.315	0.067
MnO	0.18	0.163	0.006
MgO	9.71	9.420	0.244
CaO	13.34	13.378	0.039
Na_2O	1.82	1.907	0.062
K_2O	0.03	0.016	0.005
P_2O_5	0.02	0.017	0.005

Note: Means (wt%) and standard deviations of 15 repeated analyses of the BIR–1 reference standard following Leg 152 calibration.

gas chromatography and quantified with a thermal conductivity detector. Total organic carbon (TOC) is calculated by difference between total carbon (TC) from the NCS and inorganic carbon (IC) from the coulometer:

$$TOC = TC - IC.$$

Initial Organic Matter Characterization and Determination of Maturity

Organic matter type, thermal maturity, and hydrocarbon-producing potential are assessed using a Delsi-Nermag Rock-Eval II Plus TOC instrument (Espitalié et al., 1986). The instrument uses a temperature-programmed, whole-rock pyrolysis technique to determine the amount of free hydrocarbons (S_1-Peak) and pyrolyzable hydrocarbons (S_2-Peak). The amount of CO_2 produced from the organic carbon during pyrolysis (S_3-Peak) between 300° and 390°C was trapped and measured (cf. Suess, von Huene, et al., 1988). The instrument also determines the temperature (T_{max}) of the maximal hydrocarbon formation (derived from the S_2-Peak), which is a measure of the thermal maturity of the sediment.

INORGANIC GEOCHEMISTRY

The shipboard inorganic geochemistry program for Leg 152 was focused mostly on analysis of interstitial waters extracted from 5- to 10-cm-long, whole-round sediment samples. At each site, one whole-round sample was taken from each core for the first 60 m and from every third core thereafter when sampling permitted.

Whole-round sections were cut from the cores as soon as they arrived on deck and were then capped at both ends. In the shipboard chemistry laboratory, the samples were removed from the core liner and the outside layers contaminated by drilling mud were scraped clean. The cleaned material was then placed into the standard ODP stainless-steel squeezer (Manheim and Sayles, 1974) and pressed by a Carver hydraulic press. Interstitial water was extruded into a plastic syringe and then passed through an in-line filtration apparatus into the sample bottle.

Samples were analyzed for Cl, Ca, and Mg by titration; Ca, Mg, K, and SO_4 by ion chromatography; NH_4, SiO_2, PO_4, and B by spectrophotometry; and Na, K, Sr, Mn, and Li by atomic absorption spectrophotometry. Salinity was measured with a refractometer. All analytical procedures and methodologies followed standard ODP protocol.

In addition, many samples were analyzed for the content of inorganic carbonate using routine shipboard methodologies (see also "Organic Geochemistry" section, this chapter).

Samples of interstitial waters also were retrieved from the in-situ water sampling temperature probe (WSTP) device (Fisher and Becker, 1993). These samples underwent the same scheme of analysis as the routinely obtained shipboard pore-water samples.

Table 4. Trace-element analytical precision.

Element	Published values	Mean (n = 9)	1 σ
TiO_2 (wt%)	0.96	0.94	0.02
V	312	293.99	7.06
Cr	373	336.39	3.60
Ni	166	155.97	0.68
Cu	125	128.36	2.23
Zn	70	70.48	0.92
Rb	(<1)	4.16	0.34
Sr	107	103.17	1.18
Y	16	23.49	0.16
Zr	12.7	16.46	2.40
Nb	0.5	0.68	0.22
Ba	6	11.88	3.47
Ce	2	1.24	2.07

Note: Means (ppm except for TiO_2) and standard deviations of nine repeated analyses of the BIR–1 reference standard following Leg 152 calibration.

PHYSICAL PROPERTIES

Introduction and General Objectives

The standard shipboard measurement of physical properties was expanded to include the detailed examination of those properties thought to be most sensitive to depositional environment. The principal objectives for the physical properties measurements may be grouped together as follows:

1. Relationship between the physical properties of the sediments and the environment of deposition;
2. Physical properties of the sediments with special reference to subsidence effects;
3. Assessment of geothermal conditions; and
4. Examination of the mechanical state of the volcanic pile.

To correlate shipboard and shore-based laboratory measurements with the in-situ state of stress and to develop mechanical and thermal models, the physical-properties investigations utilized the WSTP tool. Several whole-round samples from APC/XCB cored sections were taken during the cruise for onshore in-situ velocity emulation, consolidation, and strength testing.

Standard shipboard measurements of physical properties included nondestructive, whole-core, MST measurements, index properties, thermal conductivity, electrical resistivity, undrained shear strength, and compressional (*P*-) wave velocity. The latter deviated from standard procedures by including the measurement of transverse *P*-wave velocity.

Sampling Strategy

To meet our general objectives, the physical properties sampling program was formulated to fulfil several requirements:

1. To provide a comprehensive record of recovered properties. Generally, sections were scanned using the MST prior to subsampling for whole rounds. Split core samples and test locations were located at an average of two per section. When time permitted, velocimeter data were collected for three locations per section.
2. Cross-correlation with shipboard analyses. Samples were selected in conjunction with other scientists to identify features of interest. All physical properties measurements were performed on common or adjacent samples. Dried residues from index properties samples were forwarded to the chemistry laboratory for carbonate analyses, and splits from the dried portion were used for XRD mineralogical determinations. Smear-slide descriptions and grain-size analyses were targeted for the same interval as physical properties sampling. Sediment XRD samples for shore-based investigations were positioned adjacent to physical properties samples.

3. Calibration of downhole logs. Bulk density, porosity, acoustic velocity, and thermal conductivity provided identifying characteristics for log interpretation.

4. Cross-hole correlation and sediment cyclicity. MST magnetic susceptibility and natural gamma measurements were collected along the length of the unsplit cores to enable "between hole" correlation of stratigraphic horizons and to identify sediment cyclicity and turbidite events in single cores.

Laboratory Measurements

Index Properties

Index properties (bulk density, grain density, water content, porosity, and dry density) are calculated from measurements of wet and dry mass and volumes. Samples of approximately 15 cm^3 are taken for determining index properties. In addition, whole-core bulk densities are obtained from good quality, unsplit cores using the GRAPE on the MST.

Sample mass is determined aboard the ship to a precision of ±0.01 g using a Scitech electronic balance. The sample mass is counterbalanced by a known mass such that only mass differentials of less than 1 g are measured. Volumes are determined using a Quantachrome penta-pycnometer, based on the helium-displacement principle. The Quantachrome pycnometer measures volumes to an approximate precision of ±0.02 cm^3. Sample volumes are repeated until two measurements agree within the precision. A standard reference volume is run with each group of samples. The standard is rotated between cells to check for systematic error. Preliminary results suggest that the pycnometer is fairly stable for a given cell inset or sleeve. However, changing sleeves or insets can offset the standard calibration by 0.01 cm^3.

Water Content

We determined water content following the methods of the American Society for Testing and Materials (ASTM) designation D2216 (ASTM, 1989). As outlined in ASTM D2216, corrections are required for salinity when measuring marine samples. In the case of Leg 152 sediments, all pore-water salinities are within the range of 34 ± 1 ppt. In addition to the recommended water content calculation presented in ASTM D2216, which is the ratio of pore-fluid mass to the dry sediment mass (W_d = %dry wt), a calculation of the ratio of pore-fluid mass to sample mass is also reported (W_t = %wet wt). The equations for each type of water content are as follows:

$$W_d = (M_t - M_d)/(M_d - rM_t)$$

and

$$W_t = (M_t - M_d)(1 + r)/M_t,$$

where W_t = water content reported as a decimal ratio of percentage of total mass, W_d = water content reported as a decimal ratio of percentage of dry weight, M_t = total mass (saturated), M_d = dry mass, and r = salinity.

Bulk Density

Bulk density (ρ) is the density of the total sample including the pore fluid, or $\rho = M_t/V_t$, where V_t is the total sample volume. The mass (M_t) is measured using the electronic balance, and the total volume is measured with the helium pycnometer. In high-porosity sediments, the bulk density is calculated using $\rho = M_t/V_t$.

Porosity

Porosity (φ) is calculated using the equation:

$$\phi = (W_d \cdot \rho)/([1 + d]\rho_w),$$

where ρ = directly measured wet bulk density, and ρ_w = density of pore fluid.

Grain Density

The grain density (ρ_{grain}) is calculated from the dry mass (Scitech balance) and dry volume (pycnometer) measurements. Both mass and volume are corrected for salt as follows:

$$\rho_{grain} = (M_d - s)/(V_d - [s/\rho_{salt}]),$$

where V_d = dry volume, s = salt correction, ρ_{salt} = density of salt (2.257 g/cm^3), and M_d = dry mass.

A comparison of grain density with specific gravity provides a check on the various shipboard measurements. Specific gravity (G_s) was calculated using the measured bulk density and water content as follows:

$$G_s = \rho/(\rho_w[\rho - \rho_W]),$$

where ρ_w = density of pore fluid.

An initial review of the comparison between grain density and specific gravity revealed that the former is generally about 0.06 g/cm^3 less than calculated specific gravity.

Dry Density

Dry density (ρ_d) is the ratio of the dry mass (M_d) to the total volume. This value is typically used for calculating mass accumulation. Dry density is calculated for the corrected water and content and porosity for each measurement using the equation:

$$\rho_d = (\phi/W_d)\rho_w.$$

Bulk Density (Volcanics)

Bulk density (ρ) for the volcanics was calculated for all cubes and minicores cut using the double-bladed diamond saw. Dimensions of the cubes and minicores were measured with a digital caliper and then used to calculate the volume. The mass of the cube was determined using the Scitech balance.

Grain Density (Volcanics)

Cubes and minicores of known mass were placed in special sleeves in the pycnometer. This allowed the determination for the volume of solids for each cube or minicore. There is some error associated with this method, as it assumes that all pore space in the volcanics is connected and subject to helium flow.

Multisensor Track (MST)

The MST incorporates the gamma-ray attenuation porosity evaluator (GRAPE), *P*-wave logger (PWL), natural gamma, and magnetic susceptibility devices in scans of the whole-round core sections. Thermal homogeneity for the core is ensured by allowing time for the cores to equilibrate to room temperature. Geotechnical whole-round samples (15 cm) for shore-based study are removed after the entire section is scanned through the MST. Needle temperature sensors inserted into the sediment, through holes drilled in the core liner (see later), show that equilibration usually requires a 4-hr standing period. Individual unsplit core sections are then placed horizontally on the MST, which moves the section through the three sets of sensors. Geochemical whole rounds are removed on the catwalk and result in breaks in the MST data.

The GRAPE measures bulk density at 1-cm intervals by comparing attenuation of gamma rays through the cores with attenuation through an aluminum standard (Boyce, 1976). The GRAPE data are

most reliable in APC and nonbiscuited XCB and RCB cores. In biscuited material, the GRAPE is turned off on the MST. XCB and RCB drilling results in core that is of slightly smaller diameter than the calibrated core diameter. To correct for this effect, GRAPE bulk densities were corrected to discrete bulk density values from index properties samples.

The PWL transmits a 500-kHz compressional-wave pulse through the core at a repetition rate of 1 kHz. The transmitting and receiving transducers monitor the separation between the compressional-wave transducers; variations between the outside of the liner therefore do not degrade the accuracy of the velocities. Measurements are taken at 2-cm intervals. Generally, only the APC and nonbiscuited XCB and RCB cores are measured. Weak returns with signal strengths below a threshold value of 100 were removed.

Magnetic susceptibility is measured on all sections at 3-cm intervals, having a range of 0.1 on the Bartington meter, which has an 8-cm diameter loop. The close sampling is conducted to provide another measure for between-hole correlation. The quality of these results degrades in XCB and RCB sections, where the core is undersized and/or disturbed. However, the general downhole trends are used for stratigraphic correlation.

The natural gamma-ray intensity device is used to sample at 3-cm intervals; although this was time consuming, the identification of volcanic ash layers warranted the time expense. The interval was expanded when high-precision data were not required or when the precision sampling resulted in delays at the MST.

Velocimetry

Compressional-wave (*P*-wave) velocity measurements were obtained using two different systems during Leg 152, depending upon the degree of lithification of the sediments. *P*-wave velocities are measured in softer sediments using a digital sound velocimeter (DSV), known affectionately during this leg as the "Velociraptor." Velocity calculation is based on the accurate measurement of the delay time of an impulsive acoustic signal traveling between a pair of piezoelectric transducers inserted in the split sediment cores. The transducers used emit a 2-µs square wave at about 250 and 750 kHz. A dedicated microcomputer controls all functions of the velocimeter. The transmitted and received signals are digitized by a Nicolet 320 digital oscilloscope and transferred to a microcomputer for processing. The DSV software selects the first arrival (although manual selection is also available) and calculates the sediment velocity; the complete waveform is stored for calculating attenuation later.

Two transducers are used to measure the longitudinaly *P*-wave velocity. Two more transducers, orthogonal to the first set, are used to measure the transverse *P*-wave velocity. The transducers are firmly fixed at one end on a steel plate so that their separation remains as nearly constant as possible while determining velocities. At each sampling interval (usually three per section), the transducers are inserted carefully into the split section and velocities are measured in both directions.

Periodically, transducer separation is evaluated precisely by calibrating the system in distilled water. A value of sound velocity in distilled water is determined (based on standard equations) for the measured temperature, with the computer calculating the transducer separation using the signal traveltime.

The Hamilton Frame velocimeter was used to measure compressional-wave velocities at 500 kHz in discrete sediment samples when induration made it difficult to inset the DSV transducers, and in lithified sediments and basement rocks when insertion became impossible. Samples are cut carefully using a double-bladed diamond saw. Sample thickness is measured by digital calipers. Zero traveltimes for the velocity transducers are estimated by linear regression of traveltime vs. distance for a series of aluminum and lucite standards. When determining transducer traveltime, we found that the zero time was inversely related to the standard length, particularly for the lucite standard. This is likely because the lucite does not allow *P*-waves to travel as rapidly as does the aluminum, and the surface (*S*-) wave covers the distance between the transducers faster than the *P*-wave. This difference is smallest for the shortest standards, which, together with the length-dependent variation, indicates that the samples used on the Hamilton Frame should be of equal size cubes. We also found that sonic velocity varied as a function of the receiver gain. To compensate, zero-time offsets were calculated for lucite and aluminum standards at each gain setting.

Filtered seawater is used to improve the acoustic contact between the sample and the transducers. The DSV oscilloscope and processing software are used to digitize the waveforms, to calculate velocities, and to store the waveforms for calculating attenuation later. *P*-wave velocities were measured in three directions for the cubes: longitudinal (V_z: parallel to the core axis), transverse (V_x: orthogonal to the core axis and on strike to any visible bedding), and transverse (V_y: orthogonal to the core axis and downdip to any visible bedding). This approach then provides a measure of acoustic anisotropy within the sediments.

Undrained Shear Strength

The undrained shear strength of the sediments is determined using the ODP motorized miniature shear vane device, following the procedures of Boyce (1976). The vane rotation rate is set to 90°/min. Only the fine-grained, soft to stiff units are measured. The vane used for all measurements has a 1:1 blade ratio with a dimension of 1.27 cm.

The instrument measures the torque and strain at the vane shaft using a torque transducer and potentiometer, respectively. The shear strength reported is the peak strength determined from the torque vs. strain plot. In addition to the peak shear strength, the residual strength was determined from the same plot where the failure was not dominated by cracking of the sample (Pyle, 1984). In addition, remolded strength also was tested by placing the vane into the same area after the sediment had been packed back into the hole (avoiding the build-up of void spaces).

In the analysis of vane tests, the assumption is that a cylinder of sediment is sheared uniformly about the axis of the vane in an undrained condition, with cohesion as the principal contributor to shear strength. Departures from this assumption include progressive cracking within and outside of the failing core cylinder, drainage of local pore pressures (i.e., the test can no longer be considered to be undrained), and stick-slip behavior.

Electrical Resistivity

The Wayne-Kerr precision component analyzer is used to measure resistivity, following the procedures outlined in the "Explanatory Notes" chapter of the Leg 127 *Initial Reports* volume (Shipboard Scientific Party, 1990b). Electrical resistivity of the sediments is measured twice per section using a four-electrode configuration, which consists of four 2-mm stainless-steel pins with an electrode spacing of 13 mm. A 10-kHz square-wave current is applied to the outer electrodes and the difference in potential between the two inner electrodes is measured. The size of the current (typically 50 mA) is measured over a resistor in the outer circuit.

The electrodes are pushed approximately 1 cm into the split-core surface after measuring the resistance of seawater in another split liner, thus avoiding geometric differences between sediment and water samples. Most measurements are performed with the probes aligned transverse to the core axis.

Thermal Conductivity

The thermal conductivity of cored material is measured every 1.0 to 1.5 m, using the needle probe method, in full-space configuration for soft sediments (Von Herzen and Maxwell, 1959), and in half-space mode (Vacquier, 1985) for lithified sediment and hard-rock samples. All measurements are performed after the cores have equili-

brated with laboratory temperature. Data are reported in units of W/(m·K) and have an estimated error of 5% to 10%. All data have been corrected for in-situ pressure and temperature, assuming a hydrostatic pressure and a temperature gradient of 110 mK/m. The pressure correction is +1% for each 1800 m (Ratcliffe, 1960). The temperature correction is +1% for each +20°C change in temperature between the laboratory and in-situ conditions, a value intermediate between +5%, suggested by Ratcliffe (1960) for high-porosity, water-saturated sediments, and a mean value of +3%, derived from data reported by Clark (1966) for several hard rocks.

"Full-space" Measurements of Soft Sediments

Needle probes containing a heater wire and a calibrated thermistor are inserted into the sediment through small holes drilled into the core liners before the sections are split. The probes are positioned carefully where MST data indicated a sample of uniform properties. Data are acquired using a Thermcon-85 unit interfaced with an IBM PC-compatible microcomputer. This system allows one to connect and operate simultaneously up to five probes. For quality control, one probe is used with a standard of known conductivity during each run.

At the beginning of each test, temperatures in the samples are monitored without applying a heater current until the background thermal drift is determined to be less than 0.04°C/min. Once the samples have been equilibrated, the heater circuit is closed and the temperature rise in the probes is recorded. Thermal conductivities are calculated from the rate of temperature rise while the heater current is flowing.

After the heater has been on for about 60 s, the needle probe response is very near that of a line source having constant heat generation per unit of length. Temperatures recorded during a time interval of 60 to 240 s are fitted with the least-squares technique to the appropriate equation:

$$T(t) = [(q/4\pi k) \cdot \ln(t)] + L(t),$$

where k = apparent thermal conductivity, T = temperature, t = time, and q = heat input per unit length of wire per unit time.

The term $L(t)$ describes a linear change in temperature with time and includes the background temperature drift and any linearity that results from instrumental errors and the geometrical inadequacies of the experiment. These inadequacies include the finite length of the probe and sample.

All full-space measurements have been corrected for a linear offset between measured and true conductivities, determined from a series of tests with standards of known conductivities (Table 5, Fig. 10).

"Half-space" Measurements of Lithified Sediments and Hard Rock

Half-space measurements are performed on selected samples after the cores have been split, with a needle probe sandwiched between the flat surface of a test sample and that of an epoxy block, which has a relatively low conductivity (Sass et al., 1984; Vacquier, 1985). All half-space measurements are conducted in a water bath, to keep the samples saturated, to improved the thermal contact between the needle and the sample, and to reduce thermal drift during the tests.

The samples are sanded with 240- and 600-grid paper to smooth the contact area, and an EG&G thermally conductive compound is used to improve the thermal contact. Data collection and reduction procedures for half-space tests are identical to those for full-space tests.

Through tests having standards of known conductivities, correction factors are determined and taken to be linear as a first approximation, for each of three needles in the half-space bath (Table 6, Fig. 11; Lee, 1989). These corrections are specific to a fixed time interval of 60 to 240 s and account for the imperfect nature of the experiment (i.e., epoxy is not a perfect insulator; there is never an ideal thermal contact; the thermal compound may act as a heat sink; and the heat source is not positioned exactly at the boundary between the sample and epoxy).

DOWNHOLE MEASUREMENTS

Measurement Descriptions

Downhole measurements are used to directly determine the physical, chemical, and structural properties of formations adjacent to the borehole. Interpretation of these continuous, in-situ measurements can yield stratigraphic, lithologic, structural, geophysical, and geochemical characterizations of the hole. After coring is completed, a combination of sensors or tool strings is lowered down the hole on a seven-conductor cable, and each of several measuring devices continuously monitors the properties of the formations crossed by the borehole.

Two combinations of downhole sensors were used during Leg 152: (1) the geophysical combination and (2) the formation microscanner (FMS). The Lamont-Doherty Earth Observatory temperature tool was attached to the base of the geophysical combination to obtain downhole formation/fluid temperatures. The natural gamma-ray spectrometry tool (NGT) is run as part of each tool string to correlate depths between logging runs.

The geophysical combined tool string used during Leg 152 consisted of the sonic digital tool (SDT) for measuring sonic velocities, the dual induction tool (DIT) for measuring electrical resistivity, the high-temperature lithodensity tool (HLDT) for measuring formation bulk density and photoelectric effect (PEF), along with a borehole caliper measurement and the natural gamma-ray spectrometry tool (NGT).

The FMS is a microelectrical imaging device. It allows for visual characterization of the structures met in the near vicinity of the borehole wall from measurements related to the formation electrical conductivity. The FMS tool string used during Leg 152 consisted of an NGT, a general purpose inclinometer tool (GPIT), and the FMS. The FMS and GPIT provide spatially oriented microresistivity images of the borehole wall as well as a caliper measurement.

The data from the geophysical combination and FMS logging combinations are recorded by Schlumberger's new MAXIS 500 digital logging unit (deployed during Leg 149). Data from the MAXIS 500 are generated in a new data format (DLIS, digital log information standard). This is converted to LIS format (log information standard) for compatibility with on board and shore-based logging software. The Lamont temperature logging tool (TLT) data are recorded within the temperature tool, and later restored and processed on Macintosh.

Measurement Devices

A brief description of in-situ sensors used during Leg 152 is given in the following sections. A more detailed description was provided by Hearst and Nelson (1985) and Ellis (1987).

Temperature–Temperature Logging Tool (TLT)

During Leg 152, the LDEO TLT, a self-contained temperature recording tool that can be attached to any Schlumberger tool string, was used. The temperature sensors are accurately calibrated thermistors located at the lower end of the probe. Temperatures are determined from the resistance of two thermistors that can be monitored separately, or in combination for maximum sensitivity. Data from the two thermistors and a pressure transducer are collected at a pre-determined rate of one sample per 0.5 to 5.0 s and stored within the tool. Following the logging run, data are transferred from the tool to a shipboard computer for analysis. A fast-response, lower accuracy thermistor is able to detect sudden temperature excursions caused by fluid flow from the formation. A slow-response, higher accuracy thermistor can be used to estimate borehole fluid temperature. If the history of drill-fluid circulation in the hole and at least two temperature logs are available (Jaeger, 1961), the post-drilling equilibrium geotherm can be estimated. Conversion to depth is based on pressure recordings from the

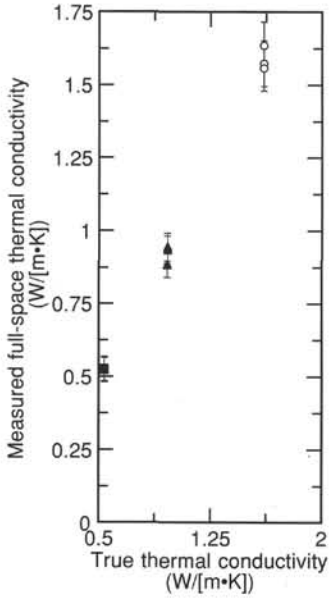

Figure 10. Standard and measured conductivities of full-space standards used during Leg 152. All data are listed in Table 6. Measured values are means and error bars showing one standard deviation. The line is a least-squares best fit, defined by the equation shown, used to correct all full-space measurements. Black rubber (solid squares); red rubber (solid triangles); Makor (open circles).

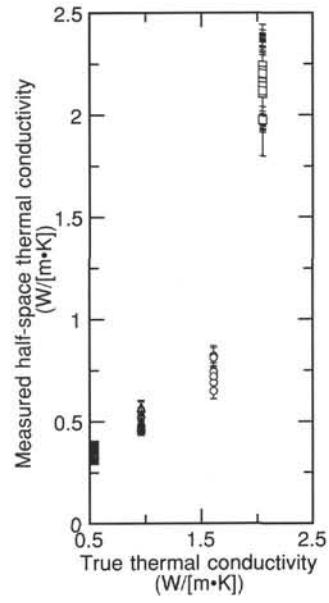

Figure 11. Standard and measured thermal conductivities of half-space standards used during Leg 152. All data are listed in Table 5. Measured values are means with error bars showing one standard deviation. The lines are least-squares best fits, defined by the equations shown, used to correct half-space measurements. Black rubber (solid squares); red rubber (open triangles); Makor (open circles); basalt (open squares).

Table 5. Measured and known thermal conductivities of full-space standards.

Standard	True thermal conductivity	Measured full-space mean conductivity	Standard deviation	Number of readings
Black rubber	0.54	0.536	0.018	15
Red rubber	0.96	0.998	0.033	15
Macor	1.61	1.808	0.061	15

Note: Thermal conductivity determined by the divided bar method at the U.S. Geological Survey, Menlo Park, CA, Tectonophysics Branch.

Table 6. Measured and known thermal conductivities of half-space standards.

Standard	True thermal conductivity	Measured half-space thermal conductivities		
		Needle 333	Needle 322	Needle 337
Black rubber	0.54	0.372 0.005 (9)	0.348 0.024 (9)	0.355 0.003 (9)
Red rubber	0.96	0.519 0.008 (8)	0.511 0.042 (9)	0.499 0.021 (9)
Macor	1.61	0.874 0.013 (9)	0.738 0.066 (6)	0.857 0.069 (9)
Basalt	2.05		2.154 0.019 (31)	

Notes: Data for each probe include mean, standard deviation, and number of measurements. True thermal conductivity determined by the divided bar method at the U.S. Geological Survey, Menlo Park, CA, Tectonophysics Branch.

pressure transducer and from the Schlumberger unit elapsed time (ETIM) records.

Electrical Resistivity–Dual Induction Tool (DIT)

The DIT provides three different measurements of electrical resistivity, each having a different depth of investigation in the formation. Two induction devices (deep and medium resistivity) transmit high-frequency alternating currents through transmitter coils, creating magnetic fields that induce secondary (Foucault) currents in the formation. These ground-loop currents produce new inductive signals, proportional to the conductivity of the formation, which are measured by the receiving coils. The measured conductivities then are converted to resistivity. A third device, a spherically focused resistivity instrument, measures the current necessary to maintain a constant voltage, which is dropped across a fixed interval.

To a first-order approximation, resistivity responds to the inverse square root of porosity (Archie, 1942). Water salinity, clay content, and temperature are important factors for controlling the electrical resistivity of rocks. Other factors that may influence the resistivity of a rock include the concentration of hydrous and metallic minerals and the abundance and geometry of interconnected pore spaces.

Sonic Velocity–Sonic Digital Tool (SDT)

Sonic tools measure the difference in compressional-wave traveltimes between a transmitter and receiver. This provides a direct measure of vertical traveltime of sound in the adjacent formation (the interval traveltime [ΔT]). The SDT is used to calculate the porosity of the formation and sonic velocity. Together, the sonic velocity and density data are used to calculate an impedance log. A synthetic seismogram then is produced from the impedance log for comparison with site-specific seismic reflection profiles.

The SDT is aimed at maximizing the information obtained from measured sonic waveforms by acquiring a digitized, complete sonic waveform downhole. This is achieved by using two transmitters and receivers having a 1-m spacing, in addition to a linear array of eight receivers spaced at 15 cm, with a transmitter-receiver distance starting at 3.33 m. The addition of a linear array in place of two discrete receivers is the main change in the SDT from earlier tools. The digitally recorded complete waveform is used post-cruise to determine shear wave and Stoneley wave velocities in addition to the real-time compressional velocity. Standard vertical resolution is 60 cm, although special array processing can produce a resolution of 15 cm.

Lithodensity Measurement–High-temperature Lithodensity Tool (HLDT)

The HLDT uses a ^{137}Ce gamma-ray source and measures the resulting gamma-ray flux at fixed distances from the source. Under normal operating conditions, attenuation of gamma rays is primarily caused by Compton scattering, which is related to electron density. Formation density is inferred from this gamma-ray flux by assuming (1) a direct relationship between electron density and bulk density and (2) that the ratio of atomic weight and the atomic number for most common rock-forming elements is constant (about 2:1).

The photoelectric absorption effect is used as an indicator of matrix lithology that is independent of porosity. Photoelectric absorption occurs at gamma-ray energies below which Compton scattering can usually occur (<100 keV). Besides being energy dependent, the probability of photoelectric absorption occurring depends on the atomic number of a formation (e.g., more sensitive to elements having higher atomic numbers). The magnitude of this measurement thus is related to the abundance of the heavier "matrix" (mineral) portion of a formation, and for this reason, it is almost entirely independent of porosity. The radioactive source and detector array are placed in a tool that is pressed against the borehole wall by a strong spring arm. Excessive roughness of the hole will cause some drilling fluid to infiltrate between the detector and the formation. As a consequence, density readings can be artificially low. Approximate corrections can be applied using caliper data.

Natural Gamma-Ray Measurement–Natural Gamma-Ray Spectrometry Tool (NGT)

The NGT measures the natural radioactivity of the formation. Most gamma rays are emitted by the radioactive isotope ^{40}K and radioactive isotopes of the U and Th decay series. The gamma-ray radiation originating in the formation close to the borehole wall is measured by a scintillation detector mounted inside the sonde. The analysis is achieved by subdividing the entire incident gamma-ray spectrum into five discrete energy windows. The total counts recorded in each window, for a specified depth in the well, are processed at the surface to give elemental abundances of K (wt%), U (ppm), and Th (ppm). The NGT also provides a measure of the total gamma-ray signature (spectral gamma-ray [SGR] or [K + U + Th]) and a uranium-free measurement (computed gamma-ray [CGR] or [Th + K]).

The natural gamma-ray measurement is commonly used to estimate the clay or shale content resulting from the relatively high abundances of radioactive elements in clay minerals. There are rock matrices, however, for which the radioactivity ranges from moderate to extremely high values as a result of the presence of volcanic ash, potassic feldspar, or other radioactive minerals.

Electrical Images of the Borehole–Formation Microscanner (FMS)

The FMS produces high-resolution borehole images from electrical conductivity measurements (Ekstrom et al., 1986). Designed for exploring for oil in the early 1980s, the use of the FMS was initially precluded in the Ocean Drilling Program because of diameter constraints imposed by the internal diameter of the drill pipe (4.125 in.). A modified, smaller-diameter sensor was consequently developed by Schlumberger for ODP. The FMS has a vertical resolution of approximately 1.0 cm, but a detection threshold for conductive features on the order of micrometers. With this fine-scaled detection ability (raw data points are recorded every 2.5 mm), the tool allows for detailed study of subsurface structures. This compares with typical conventional downhole measurements that are averaged over 150 mm; the sampling rate of the FMS, consequently, is 60 times larger than most other logging devices. The FMS has four orthogonal pads that are pressed against the borehole wall.

The ODP sensor was designed in such a way that each of the four pads carries an array of 16 closely spaced electrodes. The electrode currents probe the conductivity of the rock to a depth of a few centimeters into the borehole wall, thus responding to such variations in physical and chemical properties of the rock as porosity or surface conduction when conductive clay minerals (such as smectites) are present. The series of conductivity traces are displayed side by side, then coded into an image where dark colors represent the most conductive values and light colors the most resistive ones. The four images (of 16 traces each) are recorded simultaneously. Once the data have been acquired in the borehole, the images are processed on a dedicated workstation to allow for on-site comparison with the cores. Possible applications of the FMS-derived images include detailed core-log integration, orientation of cores, identification and mapping of fractures, faults, foliations, as well as determining strike and dip of structures (Pezard and Luthi, 1988).

The FMS may also be used to determine in-situ principal horizontal stress directions from the precise measurement of two orthogonal calipers. In an isotropic, linearly elastic rock subject to differential stresses, breakouts form along the borehole wall are a result of compressive stress concentrations that exceed the strength of the rock. Under these conditions, the breakout orientation develops in the direction of least-principal horizontal stress. It has been demonstrated in different areas that stress orientations deduced from breakouts are consistent with other independent indicators (Bell and Gough, 1979; Morin et al., 1990).

Borehole Inclination and Magnetometer Measurement–General Purpose Inclination Tool (GPIT)

Included within the FMS tool, the GPIT contains a three-component accelerometer and a three-component magnetometer. The device is used to measure the orientation of the downhole sensors within the borehole and the orientation (or deviation) of the borehole itself, as well as to compensate for instrument accelerations in the axis of the borehole while acquiring data. From the three-axis magnetometer data, a derivation of the magnetic inclination, declination and total field can be obtained, especially in basement.

Data Quality

Downhole data quality may be seriously degraded in excessively large diameter sections of the borehole or by rapid changes in the hole diameter (especially density readings and electrical images). Electrical resistivity is less sensitive to such borehole effects. The nuclear measurements (density and natural gamma ray) are most seriously impaired because of the large attenuation by the borehole fluid, although corrections can be applied to the original data to reduce the effects of these conditions.

By placing the NGT on each string, data can be depth-correlated between logging runs. Logs from different tool strings, however, may still have minor depth mismatches caused either by cable stretch or ship's heave during recording. Small errors in depth-matching can impair the multilog analyses in zones of rapidly varying lithology. Ship's heave is minimized by a hydraulic wireline heave compensator designed to adjust for rig motion during logging operations. Precise depth-matching of logs with cores is possible but difficult in zones where core recovery is low because of the inherent ambiguity of placing the recovered section within the cored interval.

Log Processing and Analysis

During each logging run, incoming data are observed in real time on a monitor in the MAXIS logging unit and simultaneously recorded on disk. After logging, data are processed and reformatted on board the ship to display the preliminary downhole measurements.

Additional conventional log processing and display were performed post-cruise by the Borehole Research Group (BRG), using Schlumberger "Logos" software and additional programs developed by members of the BRG. Displays of most of these processed data appear with accompanying text at the end of the appropriate site chapter in this volume.

Shore-based processing of data from each hole consisted of (1) depth adjustments of all logs to a common measurement below the sea floor; (2) corrections specific to certain tools; and (3) quality control and rejection of unrealistic values.

The depth-shifting procedure is based on a interactive, graphical depth-match program that allows the processor to correlate logs visually and to define appropriate shifts. The reference log and the log to be adjusted in depth are displayed side-by-side on a screen, and vectors connect the two at positions chosen by the user. The total spectral gamma-ray curve (SGR) from the NGT tool run on each logging string was used in most cases to correlate the logging runs. In general, the reference curve is chosen on the basis of constant, low cable tension and high cable speed (tools run at faster speeds are less likely to stick and are less susceptible to data degradation caused by ship's heave). Other factors, however, such as the length of the logged interval, the presence of drill pipe, and the statistical quality of the collected data (better statistics are obtained at lower logging speeds) are also considered in the selection. A list of the amount of differential depth shifts applied at each hole is available upon request to BRG (LDEO).

Specific tool corrections were performed on the gamma-ray data to account for changes in borehole size and for the composition of the drilling fluid.

Quality control was performed by cross-correlation of all logging data. If the data processor concluded that individual log measurements represented unrealistic values, the choices were to either discard the data outright and substitute the null value of "–999.25," or identify a specific depth interval containing suspect values that must be used with caution. The latter are noted in the text that accompanies all processed log displays. Quality control of the SDT acoustic data was based on discarding any of the four independant transit time measurements that were negative or that fell outside a range of reasonable values selected by the processor.

Locally, some intervals of log data appeared unreliable (usually because of poor hole conditions) and were not processed beyond what had been done onboard the ship. In general, a large (>12 in.) and/or irregular borehole affects most recordings, particularly those that require eccentralization (CNTG, HLDT) and a good contact with the borehole wall. Hole deviation can also degrade the data; the FMS, for example, is not designed to be run in holes that are more than 10° off vertical, as the tool weight might cause the caliper to close.

FMS data are processed post-cruise using Schlumberger "Logos" software at IMT at the University of Marseille (France), under the direction of the BRG (LDEO). Analysis of the resulted FMS images can be performed post-cruise (1) to produce a detailed lithostratigraphy; (2) to detect, to map, and to identify fractures and faults; (3) to orient cores as necessary; and (4) to determine the principal horizontal stress directions (Pezard, 1990).

Files of all processed logs (including FMS, dipmeter, and BRG temperature data not shown in printed form) plus explanatory texts are included on the CD-ROM enclosed in the back pocket of this volume; a directory of the contents of the disk is found at the front of this volume.

Synthetic Seismograms

Synthetic seismograms are generated from an impedance log. The interval transit-time (from the SDT tool) and density (from the HLDT) logs are used to generate an impedance log (Gal'perin, 1974). The impedance vs. depth logs then are converted to impedance vs. two-way traveltime and convoluted with a zero-phase Ricker wavelet, with various other digitized wavelet samples acquired from the *JOIDES Resolution* seismic source, and from the seismic data acquired during the *Magnus Heinasson* site survey done in 1992. The dominant frequency of the wavelet varies, depending on the source used in the original seismic profile. The vertical resolution of a 30-Hz wavelet is generally about 15 to 30 m, but improved to 5 m for the actual site-survey data for the Leg 152 sites, depending on interval velocity; thus, reflectors cannot generally be attributed to smaller-scale lithologic horizons. The final synthetic seismogram calculated includes interbed multiples.

Ms 152IR-102